Hippocampome.org v2.0: a knowledge base enabling data-driven spiking neural network simulations of rodent hippocampal circuits

Diek W. Wheeler[1,2], Jeffrey D. Kopsick[1,2], Nate Sutton[1,3], Carolina Tecuatl[1], Alexander O. Komendantov[1], Kasturi Nadella[1,3], Giorgio A. Ascoli[1,2,3*]

[1]Center for Neural Informatics, Structures, & Plasticity; Krasnow Institute for Advanced Study; George Mason University, Fairfax, VA, USA
[2]Interdisciplinary Program in Neuroscience; College of Science; George Mason University, Fairfax, VA, USA
[3]Bioengineering Department and Center for Neural Informatics, Structures, & Plasticity; College of Engineering and Computing; George Mason University, Fairfax, VA, USA
[*]Correspondence: ascoli@gmu.edu

Abstract

Hippocampome.org is a mature open-access knowledge base of the rodent hippocampal formation focusing on neuron types and their properties. Hippocampome.org v1.0 established a foundational classification system identifying 122 hippocampal neuron types based on their axonal and dendritic morphologies, main neurotransmitter, membrane biophysics, and molecular expression. Releases v1.1 through v1.12 furthered the aggregation of literature-mined data, including among others neuron counts, spiking patterns, synaptic physiology, in vivo firing phases, and connection probabilities. Those additional properties increased the online information content of this public resource over 100-fold, enabling numerous independent discoveries by the scientific community. Hippocampome.org v2.0, introduced here, incorporates over 50 new neuron types and extends the functionality to build real-scale, biologically detailed, data-driven computational simulations. In all cases, the freely downloadable model parameters are directly linked to the specific peer-reviewed empirical evidence from which they were derived. Possible research applications include quantitative, multiscale analyses of circuit connectivity and spiking neural network simulations of activity dynamics. These advances can help generate precise, experimentally testable hypotheses and shed light on the neural mechanisms underlying associative memory and spatial navigation.

Introduction

Neuroscience knowledge continues to increase every year (Eke et al., 2022; Yeung et al., 2017), making it challenging for researchers to keep abreast of mounting data and evolving information even in their own domain of expertise. Large-scale endeavors, such as the Brain Research through Advancing Innovative Neurotechnologies (BRAIN) Initiative (Insel et al., 2013) and the European Union's Human Brain Project (Amunts et al., 2016), are contributing to this tremendous growth along with the 'long tail' of independent labs and individual scientists (Ferguson et al., 2014). A key organizing principle for neuroscience knowledge is the seminal notion of *neuron types* (Petilla Interneuron Nomenclature Group et al., 2008; Zeng and Sanes, 2017), which constitute the conceptual 'parts list' of functional circuits. The National Institutes of Health launched the BICCN (see abbreviations in Materials and Methods) to help establish a comprehensive reference of the cell type diversity in the human, mouse, and non-human primate brains (BRAIN Initiative Cell Census Network, 2021). This multi-institution collaboration is already producing innovative results (Muñoz-Castañeda et al., 2021) and actionable community resources (BICCN Data Ecosystem Collaboration, 2022).

Hippocampome.org is an open-access knowledge base of the rodent hippocampal circuit (dentate gyrus, CA3, CA2, CA1, subiculum, and entorhinal cortex) at the mesoscopic level of neuron types (Wheeler et al., 2015). This resource has proven popular and effective thanks to the adoption of a simple yet powerful classification system for defining neuron types. Specifically, a key property for the identification of neuron types in Hippocampome.org is the location of axons and dendrites across the subregions and layers of the hippocampal formation. This approch can be broadly extended to classify neurons in other brain regions and neural systems (Ascoli and Wheeler, 2016). Focusing on axonal and dendritic distributions provides two considerable advantages. First, these features mediate neuronal connectivity, thus immediately revealing the underlying blueprint of network circuitry (Rees et al., 2017). Second, they are widely used in the neuroscience community as a reliable and concrete anchoring signature to correlate electrophysiological and transcriptomic profiles (DeFelipe et al., 2013). Therefore, starting from the foundational morphology-based identification of 122 neuron types in the first release (version 1.0 or v1.0), Hippocampome.org progressively amassed an increasing amount of complementary data, such as firing patterns, molecular expression, cell counts, synaptic communication, in vivo oscilations, and connection probabilities. In all cases, the public repository provided direct links to the specific peer-reviewed empirical evidence supporting the added knowledge.

Having established a web-based integrated storehouse of hippocampal information, Hippocampome.org also expanded its scope by including data-driven computational models of neuronal excitability and synaptic signaling, as well as ties to community resources such as NeuroMorpho.Org (Akram et al., 2018), SenseLab ModelDB (McDougal et al., 2017), CARLsim (Niedermeier et al., 2022), and the Allen Brain Atlas (Jones et al., 2009). Altogether, these extensions resulted in the emergence of a complete framework for launching real-scale, biologically detailed computer simulations of the hippocampal formation. The present report thus marks a new phase in the life cycle of this community resource. Hippocampome.org v2.0, introduced here, also incorporates over 50 newly identified neuron types, updating the classification to the most recent literature findings.

The following "Description of resource" section begins with a concise, referenced overview of the neural properties collated from Hippocampome.org v1.0 through release v1.12. We then briefly describe the new neuron types and data currently being added in Hippocampome.org v2.0. Next is an abridged summary of the usage and recognition of this online portal in biomedical research. This is followed by an explanation of the latest capabilities to search, filter, and download the complete set of computational

parameters enabling quantitative connectomic analyses and spiking neural network simulations. The section concludes with an outlook of possible research applications allowed by the expansion of this scientific resource.

Description of resource

Characterizing properties of hippocampal neuron types

Hippocampome.org v1.0 (Wheeler et al., 2015) established the morphological encoding of axonal and dendritic locations and the main neurotransmitter (glutamate or GABA) as the primary determinants of neuron types in the rodents hippocampal formation. For example, a DG Basket cell (with name capitalized to indicate a formally defined neuron type) is a GABAergic cell with axon contained in the granular layer and dendrites spanning all DG layers (Figures 1A1-4). In this framework, two neurons releasing the same neurotransmitter belong to different types if the axon or dendrites of only one of them invades any of the 26 layers across 6 subregions of the hippocampal formation (hippocampome.org/morphology). In other words, neurons of the same type share the same potential inputs, outputs, and excitatory vs. inhibitory function. These properties were initially supplemented with additional empirical evidence for molecular expression of major protein biomarkers (Figure 1A5; hippocampome.org/markers) and membrane biophysics (Figure 1A6-7; hippocampome.org/electrophysiology).

Many neuronal properties and functionalities were progressively added in 12 subsequent releases (Table 1). The numerical sequencing of these Hippocampome.org versions depended on the order of peer-review and publication of the corresponding scientific reports. Here we will describe them instead in logical groupings. The first two updates enhanced the user functionality of the knowledge base. Specifically, v1.1 integrated a web-based interactive thesaurus mapping of syonyms and definitions (Hamilton et al., 2017a; hippocampome.org/find-term) to help disambiguate the many terminological inconsistencies in the neuroscience literature (Shepherd et al., 2019; Yuste et al., 2020). Release v1.2 introduced the capability to browse, search, and analyze the potential connectivity between neuron types (Rees et al., 2016; Hippocampome.org/connectivity) as derived from the compiled overlapping locations of all the presynaptic axons and postsynaptic dendrites. Transcriptomic information was greatly expanded in both v1.3 (Hamilton et al., 2017b), which incorporated in situ hybridization data from the Allen Brain Atlas (Lein et al., 2007), and v1.5 (White et al., 2020), which leveraged relational inferences interlinking the region-specific expression of two or more genes.

The quantifications of firing pattern phenotypes, such as rapid adapting spiking, transient stuttering, and persistent slow-wave bursting, in v1.6 (Komendantov et al., 2019; hippocampome.org/firing_patterns) were fitted by dynamical systems modeling (Izhikevich, 2003) in v1.7 (Venkadesh et al., 2019; hippocampome.org/Izhikevich). Although the above properties were largely measured from slice preparations, v1.9 made available measurements from *in vivo* recordings (Sanchez-Aguilera et al., 2021; hippocampome.org/in-vivo). Release v1.10 provided a compendium of cognitive function linked to specific hippocampal neurons (Sutton and Ascoli, 2021; hippocampome.org/cognome), while the v1.11 neuron type census estimated the population counts for each neuron type (Attili et al., 2022; hippocampome.org/census). Last but not least are a set of properties pertaining not to individual neuron types but to synaptic connections between a pair of pre- and post-synaptic neuron types. In particular, v1.8 calculated the synaptic probabilities and the numbers of contacts per connected pair (Tecuatl et al., 2021b; hippocampome.org/syn_probabilities), and v1.4 data mined synaptic physiology

(Moradi and Ascoli, 2020; hippocampome.org/synaptome), with conductance, time constant, and short-term plasticity values normalized by age, temperature, species, sex, and recording method in v1.12 (Moradi et al., 2022; hippocampome.org/synapse), leveraging machine learning and a phenomenological model (Tsodyks et al., 1998).

Expanding the catalog of neuron types and properties from Hippocampome.org v1.x to v2.0

The Hippocampome.org framework to classify neuron types and collate their properties allows agile content updates as new data are continuously reported in the peer-reviewed literature. For example, the description of a parvalbumin-positive DG GABAergic interneuron with axon contained in the granular layer and dendrites invading the molecular layer but not the hilus (Vaden et al., 2020) supported the definition of a new neuron type (Figures 1B1-5), referred to in Hippocampome.org v2.0 as DG Basket GRALDEN. Moreover, such an identification made it possible to univocally ascribe to this neuron type previously reported electrophysiological characteristics (Figures 1B6-7; Markwardt et al., 2011). Comprehensive literature mining following the same process expanded the Hippocampome.org v2.0 catalog with 51 new neuron types[1] across 5 of the 6 subregions of the hippocampal formation (Figure 2), including axonal-dendritic morphological patterns (Figure 2A), molecular expression (Figure 2B), and membrane biophysics (Figure 2C).

Besides identifying new neuron types, the Hippocampome.org classification system also allows the ongoing accumulation of new properties onto existing neuron types as well as the reconciliation of fragmented descriptions from scientific publications (Figure 3). For instance, converging evidence indicates that EC Layer III Pyramidal cells have axonal projections in all layers of CA1 (Deller et al., 1996; Takács et al., 2012), not just in stratum lacunosum-moleculare (SLM) as originally reported (Steward, 1976). Hippocampome.org v2.0 captures both the new extracted knowledge and the corresponding experimental evidence (Figure 3A). The annotation of neuron type-specific firing phases relative to in vivo oscillations in v1.9 highlighted a clear distinction between Superficial and Deep CA1 Pyramidal cells (Sanchez-Aguilera et al., 2021). The present release enriches that description with accompanying novel molecular markers (Figure 3B1), membrane biophysics values (Figure 3B2), and differential connectivity with other subregions and neuron types (Figure 3B3). Similarly, numerous additional firing patterns (Figure 3C) have been datamined for existing neuron types, such as adapting spiking in CA3 Basket cells and non-adapting spiking in CA3 Bistratified cells (Fidzinski et al., 2015) or transient stuttering in CA1 Radiatum Giant cells (Kirson and Yaari, 2000). Notably, this includes a novel phenotype, TSTUT.PSTUT in CA1 Interneuron Specific O-targeting QuadD cells (Chamberland et al., 2010). With this report, we also release new differential connection probabilities to various CA1 neuron type targets from traditional CA3 Pyramidal cells vs. CA3c Pyramidal cells (Figure 3D) and from DG Granule cells to mossy fiber CA3 targets (Table 2).

Quantifying the content and impact of Hippocampome.org

Over the course of subsequent releases, we have measured Hippocampome.org content using two metrics. The number of pieces of knowledge (PoK) tallies the distinct units of structured information, such as the statements that DG Granule cell axons invade the hilus or that CA1 Basket cells express parvalbumin. The pieces of evidence (PoE) are specific excerpts of peer reviewed publications (portion of text, figure, or table) or database entries (e.g., from the Allen Brain Atlas) always linked to each PoK.

[1] During peer review and until the paper is accepted for publication, new v2.0 data and functionality are available to referees and beta testers at https://hippocampome.org/php_v2/morphology.php (password: hippo)

Both PoK and PoE continued to grow with successive releases of Hippocampome.org (Figure 4A). Notably, the largest increases in PoK and PoE were related to synaptic properties (Moradi and Ascoli, 2020; Tecuatl et al., 2021b; Moradi et al., 2022). Specifically, the data underlying synaptic physiology and connection probabilities were supported by over 23,000 PoE and yielded a remarkable 500,000 PoK thanks to the normalized collection of signaling and short-term plasticity modeling parameters for multiple combinations of experimental conditions.

To assess community usage of Hippocampome.org, we tracked the number of citations of the original publication (Wheeler et al., 2015) and of the subsequent versions (Figure 4B), separating simple references from actual employment of information extracted from Hippocampome.org for secondary analyses (Table 3). At the time of this writing, year 2021 proved to be the most prolific citation-wise; however, more than a third of the releases (v1.8-12) appeared after 2021 and most PoK were added in 2022, so usage could potentially accelerate further in coming years. An early application of Hippocampome.org-sourced data used subthreshold biophysical measures, such as input resistance and membrane time constant, for multicompartmental models of signal integration and extracellular field generation (Gulyas et al., 2016). That study concluded that somatic and proximal dendritic intracellular recordings in pyramidal cells and calretinin-positive interneurons, in particular, do not capture a sizable portion of the synaptic inputs. As a recent usage example, another lab employed Hippocampome.org as the primary information resource for neuron types in DG, CA3, and CA1 (Schumm et al., 2022). They discovered that mild traumatic brain injury, in the form of alterations in spike-timing-dependent plasticity, may affect the broadband power in CA3 and CA1 and the phase coherence between CA3 and CA1.

From experimental data to biologically realistic computational models

Several key neural properties collated into Hippocampome.org have gradually transformed the site from an organized repository of hippocampal knowledge to a computational framework for launching real-scale neural network simulations. Specifically, building a data-driven circuit model of a neural system (such as the hippocampal formation or portion thereof) requires four essential quantities besides the full list of neuron types (Bahmer et al., 2023; DePasquale et al., 2023): (i) the number of neurons in each type; (ii) the input-output response function for each neuron type; (iii) the connection probability for each pair of interacting neuron types; and (iv) the unitary synaptic signals for each pair of connected neuron types (Figure 5). Of those quantities, (i) and (ii) are neuron type properties, while (iii) and (iv) are properties of directional connections, defined as a distinct pair of a presynaptic and a postsynaptic neuron type. Moreover, (i) and (iii) are structural features, while (ii) and (iv) are electrophysiological ones.

Hippocampome.org v2.0 provides estimates of the number of neurons in each neuron type (i) for both rats and mice (Figure 5A). These values were derived in a two-step process (Attili et al., 2020): first, literature mining extracted suitable quantitative relations such as the cellular density in a given layer (Attili et al., 2019), the total count of neurons expressing a certain gene, or the fraction of sampled cells with a particular morphology; second, numerical optimization of the corresponding equations yielded a complete census for all neuron types. Hippocampome.org represents the neuronal input-output response function (ii) in the form of single- and multi-compartment Izhikevich models (Figure 5B) fitted by evolutionary algorithms to accurately reproduce the observed firing behavior of each neuron type (Venkadesh et al., 2018). The connection probability (iii) from one neuron type to another (Figure 5C) was computed from measurements of the appropriate axonal and dendritic lengths in each invaded

221 subregion and layer (hippocampome.org/A-D_lengths). Additionally, users can also access the
222 presynaptic and postsynaptic path distances from the respective somata
223 (hippocampome.org/soma_distances) and the number of contacts per connected neuron pairs
224 (hippocampome.org/num_contacts). As for the synaptic communication between neurons (iv),
225 Hippocampome.org adopts the Tsodyks-Pawelzik-Markram formulation, representing unitary signals
226 and short-term plasticity with five constants for each directional pair of interacting neuron types: the
227 synaptic conductance, decay time, recovery time, facilitation time, and the utilization ratio (Tsodyks et
228 al., 1998; Moradi et al., 2022). Once again, these parameters were fitted from the experimental data
229 (Moradi and Ascoli, 2018) employing deep learning to account for (and predict the effects of) numerous
230 experimental variables (Figure 5D), including species (rat vs. mouse), sex (male vs. female), age (young
231 vs. adult), recording temperature (room vs. body), and clamping configuration (voltage vs. current).
232
233 The above description underscores the crucial interconnectedness of individually measured neuronal
234 properties forming a cohesive whole in Hippocampome.org (Figure 6). In particular, normalized
235 simulation parameters (e.g., the sensitivity of recovery variable in Izhikevich models) are derived from
236 quantitative experimental measurements, such as the spiking adaptation rate (Figure 6a). Those in turn
237 are linked to an identified neuron type based on qualitative features, like calbinin expression or laminar
238 distribution of axons and dendrites. In addition to enabling computational applications as described
239 below, such integration also allows the meta-analysis of correlations between morphological features,
240 molecular profiles, electrophysiological properties, and dynamic circuit functions. At the same time,
241 several components of Hippocampome.org are also synergistically linked to external community
242 resources (Figure 6B). For example, each neuron page links out to all three-dimensional morphological
243 reconstructions of the same cell type available in NeuroMorpho.Org (Ascoli et al., 2007), and selected
244 data from NeuroMorpho.Org were used to compute axonal and dendritic length and connection
245 probabilities. Each neuron page also links out to all computational models (including Hodgkin-Huxley,
246 stochastic diffusion, mean firing rate, etc.) involving the same cell type on ModelDB (McDougal et al.,
247 2017), while conversely ModelDB includes the Izhikevich models for all Hippocampome.org neuron
248 types. Moreover, simulation parameters from Hippocampome.org are exportable to the CARLsim
249 simulation environment (Nageswaran et al., 2009), enabling fast execution of spiking neural network
250 models optimized for GPUs. Furthermore, Hippocampome.org harnessed data from the Allen Brain Atlas
251 (Lein et al., 2007) to infer gene expression for principal neurons and cell densities for use in the neuron
252 type census.
253
254 To facilitate construction of spiking neural network simulations, Hippocampome.org v2.0 also includes a
255 new graphical user interface (GUI)[2]. With this GUI, users can download sets of simulation parameter
256 values for arbitrarily selected neuron types, a subregion of interest, or the whole hippocampal
257 formation (Figure 7). The sets consist of files for the instantiation of CARLsim simulations and a CSV
258 spreadsheet of parameters for use in a different simulation environment of the user's choice. For the
259 convenience of users interested in simplified circuit models, Hippocampome.org informally ranks the
260 importance of each neuron type from 1 (essential) to 5 (dispensable). For instance, a user may choose to
261 simulate only the canonical, or rank 1, neuron types of the tri-synaptic circuit and entorhinal cortex,
262 consisting of DG granule, CA3 pyramidal, CA1 Pyramidal, and MEC LII Stellate cells. When
263 Hippocampome.org is missing a parameter value due to insufficient experimental evidence, the GUI
264 exports a default value clearly indicating so in the downloadable files. For missing Izhikevich and
265 synaptic signaling parameters, the default values are those provided by the CARLsim simulation

[2] During peer review and until the paper is accepted for publication, new v2.0 data and functionality are available to referees and beta testers at https://hippocampome.org/php_v2/simulation_parameters.php (password: hippo)

environment. For missing synaptic probabilities, Hippocampome.org stored precomputed values averaged by connection type, namely excitatory-excitatory (0.0117), excitatory-inhibitory (0.0237), inhibitory-excitatory (0.00684), and inhibitory-inhibitory (0.00423).

Potential applications to connectomic analyses and spiking neural networks simulations

Hippocampome.org v2.0 enables the multiscale analysis of circuit connectivity (Figure 8). At the highest echelon are the connections between hippocampal subregions, which are comprised of the mesoscopic level potential connectivity between individual neuron types (Figure 8A). Expanding, for example, upon the 147 connections between DG and CA3 neuron types reveals all the connections every individual neuron type forms with the other neuron types within and across the subregions (Figure 8B). Zooming in onto a single neuron type each from DG and CA3, it is possible to quantify the efferent and afferent connections with other neuron types from throughout the hippocampal formation in terms of synaptic probabilities and number of neuronal partners (Figure 8C). Diving even deeper into the isolated connection between two neuron types, such as the mossy fiber contacts from DG Granule cells to CA3 Basket cell, expands the connectivity analysis to several physiological factors affecting neuronal communication: the subcellular location of the synaptic contact (e.g., soma in stratum pyramidale and proximal dendrites in stratum lucidum), the transfer function (product of synaptic conductance and decay time constant), the in vivo firing rate of the presynaptic neuron type, and the relationship between input current and resulting output spiking frequency (F-I curve) of the post-synaptic neuron (Figure 8D).

Release of v2.0 makes the original objective of Hippocampome.org, to enable data-driven spiking neural network simulations of rodent hippocampal circuits (Ascoli, 2010), finally achievable. An ongoing line of research in this regard focuses on a real-scale mouse model of CA3, with the eventual goal of investigating the cellular mechanism of pattern completion. Initial work included excitatory Pyramidal cells and seven main inhibitory interneuron types: Axo-axonic, Basket, Basket CCK+, Bistratified, Ivy, Mossy Fiber-Associated ORDEN, and QuadD-LM (Kopsick et al., 2022). Use of Hippocampome.org parameters for cell census, Izhikevich models, synaptic signals, and connection probabilities resulted in robust, realistic, rhythmic resting state activity for all neuron types (Figure 9A). Another pursuit seeks to replicate the spatial representation in grid cells (Sargolini et al., 2006), modeled utilizing the Hippocampome.org MEC LII Stellate cells and supported by various GABAergic interneuron types (Dhillon and Jones, 2000). This study aims to reproduce the in vivo firing of these neuron types as a virtual rodent explores an open field (Figure 9B). While preliminary, these illustrative examples highlight the potential of Hippocampome.org-enabled data-driven spiking neural network simulations to investigate computational theories of cognitive functions in hippocampal circuits at the level of biologically detailed mechanisms (Sutton and Ascoli, 2021).

Discussion

Hippocampome.org, through its continuous updates and conspicuous usage, has established itself prominently amongst other readily accessible, evidence-based, expert-curated bioscience public resources of note, such as FlyBase for *Drosophila* molecular biology (The FlyBase Consortium, 1994; dos Santos et al., 2015), WormBase for nematode genomics (Stein et al., 2001), the Blue Brain Project for somatosensory cortex (Markram, 2006), SynGO for synaptic functions (Koopmans et al., 2019), and RegenBase for spinal cord injury biology (Callahan et al., 2016).

The growth of Hippocampome.org since the initial release of v1.0 (Wheeler et al., 2015) has been prodigious. To date, the site has been visited over 136,000 times with over 33,000 unique visits, and the original publication has been cited more than hundred times. Each successive release of Hippocampome.org has added new dimensions of knowledge and/or functionality and has been building toward assembling all the components necessary to produce real-scale computational models of the rodent hippocampal formation. The culmination of all this work is the release of v2.0, which introduces a framework for launching computer simulations directly from the accumulated knowledge. However, achieving simulations does not mark the end point for this project, because Hippocampome.org will continue to aggregate new knowledge as it is published in the peer-reviewed literature. Gradually, the focus of this resource will shift from development to exploitation through the in silico emulation of complex dynamics observed in vivo and in vitro, with the goal of shedding light on the underlying synaptic-level computational mechanisms.

The creation of real-scale spiking neural network models of the hippocampal formation and its subregions can foster biologically realistic, data-driven, mesoscopic simulations of cognitive function and dysfunction (Sutton and Ascoli, 2021). For instance, simulations with Hippocampome.org's real-scale model of the dentate gyrus can build on previous network models of epileptogenesis (Dyhrfjeld-Johnsen et al., 2007) by providing further clarity to the roles of all documented neuron types and their corresponding potential connections in seizure initiation and propagation. Furthermore, network models involving multiple subregions can open new vistas on unexplored territories, such as the use of real-scale models of the entorhinal cortex and CA2 to simulate the neuron- and connection-type specific mechanisms of social memory (Lopez-Rojas et al., 2022). Moreover, open source sharing of the real-scale models replicating those functions (Gleeson et al., 2017) will facilitate cross-talk within the systems neuroscience community to better understand the role of distinct neuron types in hippocampal function.

A notable aspect of Hippocampome.org is that all freely downlodable model parameters are directly linked to the specific peer-reviewed empirical evidence from which they were derived. Thus, if users disagree with a specific interpretation, or are not fully convinced by an individual experimental measurement, they maintain control in selecting the information sources. Conversely, researchers can choose to reuse the collated experimental data to constrain different computational models they may prefer, such as adopting the Hodgkin-Huxley formalism instead of Izhikevich dynamics. At the same time, Hippocampome.org is not only a collection of model parameters and corresponding empirical evidence, but it also provides an opportunity to unearth knowledge gaps, as facilitated by an intuitive search functionality (hippocampome.org/find-neuron). Missing data can serve to guide the design of targeted "low hanging fruit" experiments or to generate new hypotheses.

Another important element of Hippocampome.org is the careful annotation of the experimental metadata for each piece of evidence, including the species (rat or mouse), sex (male or female), age (young or adult) as well as any and all reported details that could affect the recorded neuronal property. Examples of these confounding factors abound especially for in vitro electrophysiological data, such as the exact chemical composition of the solution in the electrode and in the bath, slice thickness and orientation, clamping configuration, recording temperature, and animal weight. Because these covariates, when reported by the original investigators, are also stored in the database, it is possible to account for them in subsequent analyses and simulations. Hippocampome.org therefore constitutes a considerably rich one-stop resource to compare and "translate" key parameters, such as the amplitude and duration of a synaptic signal between two specifically identified neuron types, for instance, from 14 day old male rat at 22 ˚C in voltage clamp to a 56 day old female mouse at 32 ˚C in current clamp. When

fed into spiking neural network simulations, these differential parameter values can foster intuition while attempting to reconcile neuroscience theories and observations.

Hippocampome.org is yet poised for the onset of an information deluge from current and future big science projects. Although morphological identification will continue to play a fundamental role in defining neuron types and circuit connectivity, the manner in which knowledge is cross-referenced in this resource will allow its effective linkage to rapidly accumulating molecular and imaging data. The ongoing spatial transcriptomics revolution is already transforming the frontiers of cellular neuroscience, often using the hippocampus as favorite sandbox (Lein et al., 2017; Yao et al., 2021; Zeisel et al., 2015). Single-cell transcriptomics via scRNAseq can bolster the current morphological information by offering distinct transcription factor codes for existing neuron types and assist in defining new ones (Cembrowski and Spruston, 2019; Winnubst et al., 2020; Yuste et al., 2020). From the functional side, optical imaging via genetically encoded voltage indicators (Knöpfel and Song, 2019) will provide in vivo voltage traces for defined neuron types that can greatly enhance the repertoire of firing pattern phenotypes to utilize in simulations (Adam et al., 2019). Data-driven computational models can provide a useful conceptual bridge between molecular sequencing and activity imaging by investigating the effects of specific subcellular distributions of voltage- and ligand-gated conductances on neuronal excitability (Migliore et al., 2018). With the converging maturation of these young techniques and the advent of others yet on the horizon, Hippocampome.org will be able to integrate multidimensional knowledge on the solid foundation of neuronal classification.

Materials and Methods

Hippocampome.org v2.0 vs. the legacy status of v1.12

With the release of v2.0 of Hippocampome.org upon publication of this article, v1.12 of the website will no longer be updated and will transition to legacy status (hippocampome.org/legacy_v1). In this way, users may avail themselves of the full benefits of the new content and functionality of v2.0, while maintaining access to reference content as published through v1.12. In the near term, neuron types new to v2.0 are tagged with an asterisk on the web site to differentiate them from v1.1x types.

Linking neuron types to NeuroMorpho.Org morphological reconstructions

Hippocampome.org neuron types are regularly linked to appropriately identified digital reconstructions of neuronal morphology from NeuroMorpho.Org (Ascoli et al., 2007). Identification of suitable reconstructions with individual neuron types depends on the correspondence of dendritic and axonal locations across hippocampal subregions and layers, as they appear in the reference publication. Alternatively, direct cell typing by the authors in the reference publication text is accepted as evidence for canonical (principal cell) types, such as CA1 pyramidal cells or DG granule cells. Reconstructions are not linked to a neuron type if the experimental conditions are inconsistent with the inclusion criteria of Hippocampome.org, as in the case of cell cultures or embryonic development. Lack of either axonal or dendritic tracing also disqualifies reconstructions of non-canonical neurons from being linked.

Connections from DG Granule cells to CA3

To compute estimates of connection probabilities and numbers of contacts per connected pair for the rat mossy fiber-CA3 circuit, we used previously calculated average convex hull volume (Tecuatl et al.,

2021b) and several measurements from a seminal anatomical study (Acsády et al., 1998): DG Granule cell axonal length within CA3 (3,236 µm), inter-bouton distances for mossy boutons on Pyramidal cell targets in CA3c (162 µm) and in the rest of CA3 (284 µm), and inter-bouton distances for en-passant and filipodia boutons onto CA3 interneurons (67.4 µm, considering that 48 interneurons can be contacted by a single GC). Given that the mossy fibers innervate mainly CA3 SL, and due to the lack of information regarding the exact proportion of axons innervating CA3 SP, these calculations assume that GCs only innervate SL. The probabilities of connection and numbers of contacts per connected pair (Table 2) are estimated as previously described (Tecuatl et al., 2021a) utilizing the CA3 dendritic lengths reported in Hippocampome.org.

Connections from CA3 and CA3c Pyramidal cells to CA1

To compute estimates of connection probabilities and numbers of contacts per connected pair for the rat Schaffer collaterals-CA1 circuit, we utilized previously reported values for the distinct axonal innervation patterns (Ropireddy et al., 2011; Sik et al., 1993; Wittner et al., 2007) in CA1 SR and SO from CA3 Pyramidal cells (27.5% of total axonal length: 64% to SR, 15% to SP, 21% to SO) and CA3c Pyramidal cells (64.1% of total axonal length: 94% to SR, 3% to SP, 3% to SO). In addition, we used the average inter-bouton distance reported for the Schaffer collaterals (Li et al., 1994) in SR (4.47 µm) and SO (5.8 µm). Total axonal length was measured with L-Measure (Scorcioni et al., 2008) from three NeuroMorpho.Org reconstructions for CA3c (NMO_00187, NMO_00191) and CA3b (NMO_00931). We extracted parcel-specific convex hull volumes from Janelia MouseLight (Winnubst et al., 2019) Pyramidal cell reconstructions (AA0304, AA0307, AA0420, AA0960, AA0997, AA0999, AA1548) mapped to the 2022 version of the Allen Institute Common Coordinate Framework (CCF). The probabilities of connection and number of contacts per connected pair were estimated as previously described (Tecuatl et al., 2021a) using CA1 dendritic lengths from Hippocampome.org. We used separate values for inter-bouton distances in CA1 SR for CA3c Pyramidal cells (5.5 µm: Wittner et al., 2007) and CA3 Pyramidal cells (3.7 µm: Shepherd et al., 2002; 4.4 µm: Li et al., 1994; 4.29 µm: Sik et al., 1993; averaged as 4.1 µm).

Constructing Hippocampome.org spiking neural simulations

Hippocampome.org utilizes CARLsim (Nageswaran et al., 2009) as its default simulation environment (socsci.uci.edu/~jkrichma/CARLsim/). CARLsim is a graphics processing unit (GPU)-accelerated library of functions for simulating spiking neural networks based on Izhikevich neuron models (Izhikevich, 2003). The current version is CARLsim 6 (Niedermeier et al., 2022), and the most up-to-date Hippocampome.org-optimized code base, including features not yet released in the main CARLsim version, can be found at hippocampome.org/CARLsim (Kopsick et al., 2022).

Web portal, database, and source code

Hippocampome.org runs on current versions of Chrome, Safari, and Edge web browsers, and it is deployed on a CentOS server running Apache. The website runs off of PHP from a MySQL database. The code for Hippocampome.org is available open source at github.com/Hippocampome-Org. This includes all code for displaying the pages of the website, all scripts for importing spreadsheets into the database, code for using evolutionary algorithms to optimize Izhikevich model parameters, code for the graph theory analysis of the potential connectome, code for the implementation of the firing pattern classification algorithm, and code for analyzing network simulations in CARLsim.

Glossary of abbreviations

5HT-3:	serotonin receptor 3
AA:	EC LII Axo-axonic cell
AAC:	Axo-axonic cell
ABA:	Allen Brain Atlas
AP_{ampl}:	action potential amplitude
AP_{width}:	action potential width
ASP.:	adapting spiking
Astn2:	astrotactin 2
BC:	Basket cell
BC MP:	EC LII Basket-Multipolar cell
BiC:	Bistratified cell
BICCN:	BRAIN Initiative Cell Census Network
C:	Capacitance
CB:	calbindin
CB1:	cannabinoid receptor type 1
CCK+:	cholecystokinin-positive
CR:	calretinin
CSV:	comma-separated value
Dcn:	decorin
DG:	dentate gyrus
E-E:	excitatory to excitatory
E-I:	excitatory to inhibitory
EC:	entorhinal cortex
ENK:	enkephalin
fAHP:	fast after-hyperpolarizing potential
g:	conductance constant
GABAa α1:	GABA-a alpha 1 subunit
GC:	granule cell
Gpc3:	glypican 3
GPUs:	graphical processing units
GRALDEN:	GRAnule-Like DENdrites
Garci:	grid cell
Grp:	gastrin releasing peptide
GUI:	graphical user interface
H:	hilus
HIPROM:	Hilar Interneuron with PRojections to the Outer Molecular layer
Htr2c:	5-hydroxytryptamine receptor 2c
I-E:	inhibitory to excitatory
I-I:	inhibitory to inhibitory
IS:	interneuron specific
LI-II:	layers 1-2
LII:	layer 2
LIII:	layer 3
Max FR:	maximum firing rate
MEC:	medial entorhinal cortex
MFA:	Mossy Fiber-Associated
mGluR1a:	metabotropic glutamate receptor 1 alpha

506 MOCAP: cell with MOlecular Commissural-Associational Pathway-related axons and dendrites
507 MOLAX: MOlecular Layer Axons
508 MP PC: EC LI-II Multipolar Pyramidal cell
509 Mus2R: muscarinic type 2 receptor
510 NASP: non-adapting spiking
511 Ndst4: N-deacetylase and N-sulfotransferase 4
512 nNOS: neuronal nitric oxide synthase
513 Nov: nephroblastoma overexpressed
514 NPY: neuropeptide Y
515 Nr3c2: nuclear receptor subfamily 3 group C member 2
516 Nr4a1: nuclear receptor subfamily 4 group A member 1
517 ORAX; ORiens AXons
518 ORDEN: ORiens DENdrites
519 PC: pyramidal cell / CA1 Pyramidal cell (Fig. 9B)
520 PL: polymorphic layer
521 PoE: pieces of evidence
522 PoK: pieces of knowledge
523 Prss12: serine protease 12
524 Prss23: serine protease 23
525 PV+: parvalbumin-positive
526 QuadD-LM: quadrilaminar dendrites – lacunosum-moleculare
527 R_{in}: input resistance
528 RLN: reelin
529 sAHP: slow after-hyperpolarizing potential
530 SC: MEC LII Stellate cell
531 SD: standard deviation
532 SG: stratum granulosum
533 SL: stratum lucidum
534 SLM: stratum lacunosum-moleculare
535 SMi: inner stratum moleculare
536 SMo: outer stratum moleculare
537 SO: stratum oriens
538 SOM: somatostatin
539 SP: stratum pyramidale
540 SR: stratum radiatum
541 Sub: subiculum
542 SWR: sharp-wave ripple
543 SynGO: synaptic gene ontologies
544 T: Temperature
545 τ_d: synaptic decay constant
546 τ_f: facilitation time constant
547 τ_m: membrane time constant
548 τ_r: recovery time constant
549 TPM: Tsodyks-Pawelzik-Markram
550 TSTUT.: transient stuttering
551 TSTUT.PSTUT: transient stuttering followed by persistent stuttering
552 TSTUT.SLN: silence preceded by transient stuttering
553 U: utilization ratio

554 vGluT3: vesicular glutamate transporter 3
555 V_h: holding potential
556 VIP: vasoactive intestinal polypeptide
557 V_{min}: post-spike reset potential
558 V_{peak}: spike cutoff potential
559 V_r / V_{rest}: resting membrane potential
560 V_t / V_{thresh}: firing threshold potential
561 WA BC: Wide-arbor Basket cell
562 Wfs1: wolframin ER transmembrane glycoprotein
563
564 **Acknowledgements**
565
566 We thank David J. Hamilton, Charise M. White, Christopher L. Rees, Maurizio Bergamino, Keivan Moradi,
567 Siva Venkadesh, Alberto Sanchez-Aguilera, Teresa Jurado-Parras, Manuel Valero, Miriam S. Nokia, Elena
568 Cid, Ivan Fernandez-Lamo, Daniel García-Rincón, Liset M. de la Prida, Sarojini M. Attili, Iqbal Addou, and
569 the many student interns (hippocampome.org/thx) for invaluable help advancing from v1.0 to v2.0.
570
571 **Competing Interests**
572
573 The authors have no competing interests.
574
575 **Contributions**
576
577 DWW contributed to the conceptualization, methodology, software, investigation, data curation, writing
578 – original draft, visualization, supervision, and project administration. JDK contributed to the
579 methodology, software, formal analysis, investigation, data curation, and writing – review and editing.
580 NS contributed to the methodology, software, investigation, data curation, writing – review and editing,
581 and visualization. CT contributed to the methodology, validation, formal analysis, investigation, data
582 curation, writing – review and editing, visualization, and supervision. AOK contributed to the formal
583 analysis, writing – review and editing, and visualization. KN contributed to the software and writing –
584 review and editing. GAA contributed to the conceptualization, methodology, resources, investigation,
585 data curation, writing – review and editing, visualization, supervision, project administration, and
586 funding acquisition.
587
588 **Funding information**
589
590 This work was supported in part by grants R01NS39600, RF1MH128693, and U01MH114829 from the
591 National Institutes of Health (NIH), and DE-SC0022998 from the Department of Energy (DOE). The
592 funding sources were not involved in study design, data collection and interpretation, or the decision to
593 submit the work for publication.
594

References

Acsády L, Kamondi A, Sík A, Freund T, Buzsáki G. 1998. GABAergic cells are the major postsynaptic targets of mossy fibers in the rat hippocampus. *The Journal of Neuroscience: The Official Journal of the Society for Neuroscience* **18**:3386–3403. doi:10.1523/JNEUROSCI.18-09-03386.1998

Adam Y, Kim JJ, Lou S, Zhao Y, Xie ME, Brinks D, Wu H, Mostajo-Radji MA, Kheifets S, Parot V, Chettih S, Williams KJ, Gmeiner B, Farhi SL, Madisen L, Buchanan EK, Kinsella I, Zhou D, Paninski L, Harvey CD, Zeng H, Arlotta P, Campbell RE, Cohen AE. 2019. Voltage imaging and optogenetics reveal behaviour-dependent changes in hippocampal dynamics. *Nature* **569**:413–417. doi:10.1038/s41586-019-1166-7

Aery Jones EA, Rao A, Zilberter M, Djukic B, Bant JS, Gillespie AK, Koutsodendris N, Nelson M, Yoon SY, Huang K, Yuan H, Gill TM, Huang Y, Frank LM. 2021. Dentate gyrus and CA3 GABAergic interneurons bidirectionally modulate signatures of internal and external drive to CA1. *Cell Reports* **37**:110159. doi:10.1016/j.celrep.2021.110159

Akram MA, Nanda S, Maraver P, Armañanzas R, Ascoli GA. 2018. An open repository for single-cell reconstructions of the brain forest. *Scientific Data* **5**:180006. doi:10.1038/sdata.2018.6

Amunts K, Ebell C, Muller J, Telefont M, Knoll A, Lippert T. 2016. The Human Brain Project: Creating a European Research Infrastructure to Decode the Human Brain. *Neuron* **92**:574–581. doi:10.1016/j.neuron.2016.10.046

Ascoli GA, Donohue DE, Halavi M. 2007. NeuroMorpho.Org: a central resource for neuronal morphologies. *The Journal of Neuroscience: The Official Journal of the Society for Neuroscience* **27**:9247–9251. doi:10.1523/JNEUROSCI.2055-07.2007

Ascoli GA, Wheeler DW. 2016. In search of a periodic table of the neurons: Axonal-dendritic circuitry as the organizing principle: Patterns of axons and dendrites within distinct anatomical parcels provide the blueprint for circuit-based neuronal classification. *BioEssays* **38**:969–976. doi:10.1002/bies.201600067

Attili SM, Mackesey ST, Ascoli GA. 2020. Operations research methods for estimating the population size of neuron types. *Annals of Operations Research* **289**:33–50. doi:10.1007/s10479-020-03542-7

Attili SM, Moradi K, Wheeler DW, Ascoli GA. 2022. Quantification of neuron types in the rodent hippocampal formation by data mining and numerical optimization. *The European Journal of Neuroscience* **55**:1724–1741. doi:10.1111/ejn.15639

Attili SM, Silva MFM, Nguyen T, Ascoli GA. 2019. Cell numbers, distribution, shape, and regional variation throughout the murine hippocampal formation from the adult brain Allen Reference Atlas. *Brain Structure and Function* **224**:2883–2897. doi:10.1007/s00429-019-01940-7

Bahmer A, Gupta D, Effenberger F. 2023. Modern Artificial Neural Networks: Is Evolution Cleverer? *Neural Computation* **35**:763–806. doi:10.1162/neco_a_01575

BICCN Data Ecosystem Collaboration: Hawrylycz MJ, Martone ME, Hof PR, Lein ES, Regev A, Ascoli GA, Bjaalie JG, Dong H-W, Ghosh SS, Gillis J, Hertzano R, Haynor DR, Kim Y, Liu Y, Miller JA, Mitra PP, Mukamel E, Osumi-Sutherland D, Peng H, Ray PL, Sanchez R, Ropelewski A, Scheuermann RH, Tan SZK, Tickle T, Tilgner H, Varghese M, Wester B, White O, Aevermann B, Allemang D, Ament S, Athey TL, Baker PM, Baker C, Baker KS, Bandrowski A, Bishwakarma P, Carr A, Chen M, Choudhury R, Cool J, Creasy H, D'Orazi F, Degatano K, Dichter B, Ding S-L, Dolbeare T, Ecker JR, Fang R, Fillion-Robin J-C, Fliss TP, Gee J, Gillespie T, Gouwens N, Halchenko YO, Harris N, Herb BR, Hintiryan H, Hood G, Horvath S, Jarecka D, Jiang S, Khajouei F, Kiernan EA, Kir H, Kruse L, Lee C, Lelieveldt B, Li Y, Liu H, Markuhar A, Mathews J, Mathews KL, Miller MI, Mollenkopf T, Mufti S, Mungall CJ, Ng L, Orvis J, Puchades MA, Qu L, Receveur JP, Ren B, Sjoquist N, Staats B, Thompson CL, Tward D, Van Velthoven CTJ, Wang Q, Xie F, Xu H, Yao Z, Yun Z, Zeng H, Zhang G-

Q, Zhang YR, Zheng JW, Zingg B. 2022. The BRAIN Initiative Cell Census Network Data Ecosystem: A User's Guide. PLoS Biology, In Press. Preprint: doi:10.1101/2022.10.26.513573

Callahan A, Abeyruwan SW, Al-Ali H, Sakurai K, Ferguson AR, Popovich PG, Shah NH, Visser U, Bixby JL, Lemmon VP. 2016. RegenBase: a knowledge base of spinal cord injury biology for translational research. *Database: The Journal of Biological Databases and Curation* **2016**:baw040. doi:10.1093/database/baw040

Cembrowski MS, Spruston N. 2019. Heterogeneity within classical cell types is the rule: lessons from hippocampal pyramidal neurons. *Nature Reviews Neuroscience* **20**:193–204. doi:10.1038/s41583-019-0125-5

Chamberland S, Salesse C, Topolnik D, Topolnik L. 2010. Synapse-specific inhibitory control of hippocampal feedback inhibitory circuit. *Frontiers in Cellular Neuroscience* **4**:130. doi:10.3389/fncel.2010.00130

Ciarpella F, Zamfir RG, Campanelli A, Ren E, Pedrotti G, Bottani E, Borioli A, Caron D, Di Chio M, Dolci S, Ahtiainen A, Malpeli G, Malerba G, Bardoni R, Fumagalli G, Hyttinen J, Bifari F, Palazzolo G, Panuccio G, Curia G, Decimo I. 2021. Murine cerebral organoids develop network of functional neurons and hippocampal brain region identity. *iScience* **24**:103438. doi:10.1016/j.isci.2021.103438

DeFelipe J, López-Cruz PL, Benavides-Piccione R, Bielza C, Larrañaga P, Anderson S, Burkhalter A, Cauli B, Fairén A, Feldmeyer D, Fishell G, Fitzpatrick D, Freund TF, González-Burgos G, Hestrin S, Hill S, Hof PR, Huang J, Jones EG, Kawaguchi Y, Kisvárday Z, Kubota Y, Lewis DA, Marín O, Markram H, McBain CJ, Meyer HS, Monyer H, Nelson SB, Rockland K, Rossier J, Rubenstein JLR, Rudy B, Scanziani M, Shepherd GM, Sherwood CC, Staiger JF, Tamás G, Thomson A, Wang Y, Yuste R, Ascoli GA. 2013. New insights into the classification and nomenclature of cortical GABAergic interneurons. *Nature Reviews Neuroscience* **14**:202–216. doi:10.1038/nrn3444

Deller T, Adelmann G, Nitsch R, Frotscher M. 1996. The alvear pathway of the rat hippocampus. *Cell and Tissue Research* **286**:293–303. doi:10.1007/s004410050699

Depannemaecker D, Canton Santos LE, Rodrigues AM, Scorza CA, Scorza FA, Almeida A-CG de. 2020. Realistic spiking neural network: Non-synaptic mechanisms improve convergence in cell assembly. *Neural Networks: The Official Journal of the International Neural Network Society* **122**:420–433. doi:10.1016/j.neunet.2019.09.038

DePasquale B, Sussillo D, Abbott LF, Churchland MM. 2023. The centrality of population-level factors to network computation is demonstrated by a versatile approach for training spiking networks. *Neuron* **111**:631-649.e10. doi:10.1016/j.neuron.2022.12.007

Dhillon A, Jones RS. 2000. Laminar differences in recurrent excitatory transmission in the rat entorhinal cortex in vitro. *Neuroscience* **99**:413–422. doi:10.1016/s0306-4522(00)00225-6

Dyhrfjeld-Johnsen J, Santhakumar V, Morgan RJ, Huerta R, Tsimring L, Soltesz I. 2007. Topological determinants of epileptogenesis in large-scale structural and functional models of the dentate gyrus derived from experimental data. *Journal of neurophysiology* **97**:1566–1587. doi:10.1152/jn.00950.2006

Ecker A, Romani A, Sáray S, Káli S, Migliore M, Falck J, Lange S, Mercer A, Thomson AM, Muller E, Reimann MW, Ramaswamy S. 2020. Data-driven integration of hippocampal CA1 synaptic physiology in silico. *Hippocampus* **30**:1129–1145. doi:10.1002/hipo.23220

Eke DO, Bernard A, Bjaalie JG, Chavarriaga R, Hanakawa T, Hannan AJ, Hill SL, Martone ME, McMahon A, Ruebel O, Crook S, Thiels E, Pestilli F. 2022. International data governance for neuroscience. *Neuron* **110**:600–612. doi:10.1016/j.neuron.2021.11.017

Faghihi F, Moustafa AA. 2017. Combined Computational Systems Biology and Computational Neuroscience Approaches Help Develop of Future "Cognitive Developmental Robotics." *Frontiers in Neurorobotics* **11**:63. doi:10.3389/fnbot.2017.00063

690 Ferguson AR, Nielson JL, Cragin MH, Bandrowski AE, Martone ME. 2014. Big data from small data: data-
691 sharing in the "long tail" of neuroscience. *Nature Neuroscience* **17**:1442–1447.
692 doi:10.1038/nn.3838
693 Fidzinski P, Korotkova T, Heidenreich M, Maier N, Schuetze S, Kobler O, Zuschratter W, Schmitz D,
694 Ponomarenko A, Jentsch TJ. 2015. KCNQ5 K(+) channels control hippocampal synaptic inhibition
695 and fast network oscillations. *Nature Communications* **6**:6254. doi:10.1038/ncomms7254
696 Gleeson P, Davison AP, Silver RA, Ascoli GA. 2017. A Commitment to Open Source in Neuroscience.
697 *Neuron* **96**:964–965. doi:10.1016/j.neuron.2017.10.013
698 Gulyás AI, Freund TF, Káli S. 2016. The Effects of Realistic Synaptic Distribution and 3D Geometry on
699 Signal Integration and Extracellular Field Generation of Hippocampal Pyramidal Cells and
700 Inhibitory Neurons. *Frontiers in Neural Circuits* **10**:88. doi:10.3389/fncir.2016.00088
701 Hamilton DJ, Wheeler DW, White CM, Rees CL, Komendantov AO, Bergamino M, Ascoli GA. 2017a.
702 Name-calling in the hippocampus (and beyond): coming to terms with neuron types and
703 properties. *Brain Informatics* **4**:1–12. doi:10.1007/s40708-016-0053-3
704 Hamilton DJ, White CM, Rees CL, Wheeler DW, Ascoli GA. 2017b. Molecular fingerprinting of principal
705 neurons in the rodent hippocampus: A neuroinformatics approach. *Journal of Pharmaceutical*
706 *and Biomedical Analysis* **144**:269–278. doi:10.1016/j.jpba.2017.03.062
707 Hosp JA, Strüber M, Yanagawa Y, Obata K, Vida I, Jonas P, Bartos M. 2014. Morpho-physiological criteria
708 divide dentate gyrus interneurons into classes. *Hippocampus* **24**:189–203.
709 doi:10.1002/hipo.22214
710 Hunsberger MS, Mynlieff M. 2020. BK potassium currents contribute differently to action potential
711 waveform and firing rate as rat hippocampal neurons mature in the first postnatal week. *Journal*
712 *of Neurophysiology* **124**:703–714. doi:10.1152/jn.00711.2019
713 Insel TR, Landis SC, Collins FS. 2013. Research priorities. The NIH BRAIN Initiative. *Science (New York, NY)*
714 **340**:687–688. doi:10.1126/science.1239276
715 Izhikevich EM. 2003. Simple model of spiking neurons. *IEEE transactions on neural networks* **14**:1569–
716 1572. doi:10.1109/TNN.2003.820440
717 Jones AR, Overly CC, Sunkin SM. 2009. The Allen Brain Atlas: 5 years and beyond. *Nature Reviews*
718 *Neuroscience* **10**:821–828. doi:10.1038/nrn2722
719 Kirson ED, Yaari Y. 2000. Unique properties of NMDA receptors enhance synaptic excitation of radiatum
720 giant cells in rat hippocampus. *The Journal of Neuroscience: The Official Journal of the Society for*
721 *Neuroscience* **20**:4844–4854.
722 Knöpfel T, Song C. 2019. Optical voltage imaging in neurons: moving from technology development to
723 practical tool. *Nature Reviews Neuroscience* **20**:719–727. doi:10.1038/s41583-019-0231-4
724 Kohara K, Pignatelli M, Rivest AJ, Jung H-Y, Kitamura T, Suh J, Frank D, Kajikawa K, Mise N, Obata Y,
725 Wickersham IR, Tonegawa S. 2014. Cell type-specific genetic and optogenetic tools reveal
726 hippocampal CA2 circuits. *Nature Neuroscience* **17**:269–279. doi:10.1038/nn.3614
727 Komendantov AO, Venkadesh S, Rees CL, Wheeler DW, Hamilton DJ, Ascoli GA. 2019. Quantitative firing
728 pattern phenotyping of hippocampal neuron types. *Scientific Reports* **9**:17915.
729 doi:10.1038/s41598-019-52611-w
730 Koopmans F, van Nierop P, Andres-Alonso M, Byrnes A, Cijsouw T, Coba MP, Cornelisse LN, Farrell RJ,
731 Goldschmidt HL, Howrigan DP, Hussain NK, Imig C, de Jong APH, Jung H, Kohansalnodehi M,
732 Kramarz B, Lipstein N, Lovering RC, MacGillavry H, Mariano V, Mi H, Ninov M, Osumi-Sutherland
733 D, Pielot R, Smalla KH, Tang H, Tashman K, Toonen RFG, Verpelli C, Reig-Viader R, Watanabe K,
734 van Weering J, Achsel T, Ashrafi G, Asi N, Brown TC, De Camilli P, Feuermann M, Foulger RE,
735 Gaudet P, Joglekar A, Kanellopoulos A, Malenka R, Nicoll RA, Pulido C, de Juan-Sanz J, Sheng M,
736 Südhof TC, Tilgner HU, Bagni C, Bayés À, Biederer T, Brose N, Chua JJE, Dieterich DC,
737 Gundelfinger ED, Hoogenraad C, Huganir RL, Jahn R, Kaeser PS, Kim E, Kreutz MR, McPherson PS,

Neale BM, O'Connor V, Posthuma D, Ryan TA, Sala C, Feng G, Hyman SE, Thomas PD, Smit AB, Verhage M. 2019. SynGO: An Evidence-Based, Expert-Curated Knowledge Base for the Synapse. *Neuron* **103**:217-234.e4. doi:10.1016/j.neuron.2019.05.002

Kopsick JD, Tecuatl C, Moradi K, Attili SM, Kashyap HJ, Xing J, Chen K, Krichmar JL, Ascoli GA. 2022. Robust Resting-State Dynamics in a Large-Scale Spiking Neural Network Model of Area CA3 in the Mouse Hippocampus. *Cognitive Computation*. doi:10.1007/s12559-021-09954-2

Lee C-T, Kao M-H, Hou W-H, Wei Y-T, Chen C-L, Lien C-C. 2016. Causal Evidence for the Role of Specific GABAergic Interneuron Types in Entorhinal Recruitment of Dentate Granule Cells. *Scientific Reports* **6**:36885. doi:10.1038/srep36885

Lee S-H, Marchionni I, Bezaire M, Varga C, Danielson N, Lovett-Barron M, Losonczy A, Soltesz I. 2014. Parvalbumin-positive basket cells differentiate among hippocampal pyramidal cells. *Neuron* **82**:1129–44. doi:10.1016/j.neuron.2014.03.034

Lein E, Borm LE, Linnarsson S. 2017. The promise of spatial transcriptomics for neuroscience in the era of molecular cell typing. *Science* **358**:64–69. doi:10.1126/science.aan6827

Lein ES, Hawrylycz MJ, Ao N, Ayres M, Bensinger A, Bernard A, Boe AF, Boguski MS, Brockway KS, Byrnes EJ, Chen Lin, Chen Li, Chen T-M, Chin MC, Chong J, Crook BE, Czaplinska A, Dang CN, Datta S, Dee NR, Desaki AL, Desta T, Diep E, Dolbeare TA, Donelan MJ, Dong H-W, Dougherty JG, Duncan BJ, Ebbert AJ, Eichele G, Estin LK, Faber C, Facer BA, Fields R, Fischer SR, Fliss TP, Frensley C, Gates SN, Glattfelder KJ, Halverson KR, Hart MR, Hohmann JG, Howell MP, Jeung DP, Johnson RA, Karr PT, Kawal R, Kidney JM, Knapik RH, Kuan CL, Lake JH, Laramee AR, Larsen KD, Lau C, Lemon TA, Liang AJ, Liu Y, Luong LT, Michaels J, Morgan JJ, Morgan RJ, Mortrud MT, Mosqueda NF, Ng LL, Ng R, Orta GJ, Overly CC, Pak TH, Parry SE, Pathak SD, Pearson OC, Puchalski RB, Riley ZL, Rockett HR, Rowland SA, Royall JJ, Ruiz MJ, Sarno NR, Schaffnit K, Shapovalova NV, Sivisay T, Slaughterbeck CR, Smith SC, Smith KA, Smith BI, Sodt AJ, Stewart NN, Stumpf K-R, Sunkin SM, Sutram M, Tam A, Teemer CD, Thaller C, Thompson CL, Varnam LR, Visel A, Whitlock RM, Wohnoutka PE, Wolkey CK, Wong VY, Wood M, Yaylaoglu MB, Young RC, Youngstrom BL, Yuan XF, Zhang B, Zwingman TA, Jones AR. 2007. Genome-wide atlas of gene expression in the adult mouse brain. *Nature* **445**:168–176. doi:10.1038/nature05453

Li XG, Somogyi P, Ylinen A, Buzsáki G. 1994. The hippocampal CA3 network: an in vivo intracellular labeling study. *The Journal of Comparative Neurology* **339**:181–208. doi:10.1002/cne.903390204

Lopez-Rojas J, de Solis CA, Leroy F, Kandel ER, Siegelbaum SA. 2022. A direct lateral entorhinal cortex to hippocampal CA2 circuit conveys social information required for social memory. *Neuron* **110**:1559-1572.e4. doi:10.1016/j.neuron.2022.01.028

Lübke J, Frotscher M, Spruston N. 1998. Specialized electrophysiological properties of anatomically identified neurons in the hilar region of the rat fascia dentata. *Journal of Neurophysiology* **79**:1518–1534. doi:10.1152/jn.1998.79.3.1518

Luo Y-F, Ye X-X, Fang Y-Z, Li M-D, Xia Z-X, Liu J-M, Lin X-S, Huang Z, Zhu X-Q, Huang J-J, Tan D-L, Zhang Y-F, Liu H-P, Zhou J, Shen Z-C. 2021. mTORC1 Signaling Pathway Mediates Chronic Stress-Induced Synapse Loss in the Hippocampus. *Frontiers in Pharmacology* **12**:801234. doi:10.3389/fphar.2021.801234

Markram H. 2006. The blue brain project. *Nature Reviews Neuroscience* **7**:153–160. doi:10.1038/nrn1848

Markwardt SJ, Dieni CV, Wadiche JI, Overstreet-Wadiche L. 2011. Ivy/neurogliaform interneurons coordinate activity in the neurogenic niche. *Nature neuroscience* **14**:1407–1409. doi:10.1038/nn.2935

McDougal RA, Morse TM, Carnevale T, Marenco L, Wang R, Migliore M, Miller PL, Shepherd GM, Hines ML. 2017. Twenty years of ModelDB and beyond: building essential modeling tools for the

future of neuroscience. *Journal of Computational Neuroscience* **42**:1–10. doi:10.1007/s10827-016-0623-7

Mehta K, Goldin RF, Marchette D, Vogelstein JT, Priebe CE, Ascoli GA. 2021. Neuronal classification from network connectivity via adjacency spectral embedding. *Network Neuroscience (Cambridge, Mass)* **5**:689–710. doi:10.1162/netn_a_00195

Migliore R, Lupascu CA, Bologna LL, Romani A, Courcol J-D, Antonel S, Van Geit WAH, Thomson AM, Mercer A, Lange S, Falck J, Rössert CA, Shi Y, Hagens O, Pezzoli M, Freund TF, Kali S, Muller EB, Schürmann F, Markram H, Migliore M. 2018. The physiological variability of channel density in hippocampal CA1 pyramidal cells and interneurons explored using a unified data-driven modeling workflow. *PLOS Computational Biology* **14**:e1006423. doi:10.1371/journal.pcbi.1006423

Moradi K, Aldarraji Z, Luthra M, Madison GP, Ascoli GA. 2022. Normalized unitary synaptic signaling of the hippocampus and entorhinal cortex predicted by deep learning of experimental recordings. *Communications Biology* **5**:418. doi:10.1038/s42003-022-03329-5

Moradi K, Ascoli GA. 2020. A comprehensive knowledge base of synaptic electrophysiology in the rodent hippocampal formation. *Hippocampus* **30**:314–331. doi:10.1002/hipo.23148

Moradi K, Ascoli GA. 2018. Systematic Data Mining of Hippocampal Synaptic Properties In: Cutsuridis V, Graham BP, Cobb S, Vida I, editors. Hippocampal Microcircuits, Springer Series in Computational Neuroscience. Cham: Springer International Publishing. pp. 441–471. doi:10.1007/978-3-319-99103-0_11

Muñoz-Castañeda R, Zingg B, Matho KS, Chen X, Wang Q, Foster NN, Li A, Narasimhan A, Hirokawa KE, Huo B, Bannerjee S, Korobkova L, Park CS, Park Y-G, Bienkowski MS, Chon U, Wheeler DW, Li Xiangning, Wang Yun, Naeemi M, Xie P, Liu L, Kelly K, An X, Attili SM, Bowman I, Bludova A, Cetin A, Ding L, Drewes R, D'Orazi F, Elowsky C, Fischer S, Galbavy W, Gao L, Gillis J, Groblewski PA, Gou L, Hahn JD, Hatfield JT, Hintiryan H, Huang JJ, Kondo H, Kuang X, Lesnar P, Li Xu, Li Y, Lin M, Lo D, Mizrachi J, Mok S, Nicovich PR, Palaniswamy R, Palmer J, Qi X, Shen E, Sun Y-C, Tao HW, Wakemen W, Wang Yimin, Yao S, Yuan J, Zhan H, Zhu M, Ng L, Zhang LI, Lim BK, Hawrylycz M, Gong H, Gee JC, Kim Y, Chung K, Yang XW, Peng H, Luo Q, Mitra PP, Zador AM, Zeng H, Ascoli GA, Josh Huang Z, Osten P, Harris JA, Dong H-W. 2021. Cellular anatomy of the mouse primary motor cortex. *Nature* **598**:159–166. doi:10.1038/s41586-021-03970-w

Nageswaran JM, Dutt N, Krichmar JL, Nicolau A, Veidenbaum AV. 2009. A configurable simulation environment for the efficient simulation of large-scale spiking neural networks on graphics processors. *Neural Networks: The Official Journal of the International Neural Network Society* **22**:791–800. doi:10.1016/j.neunet.2009.06.028

Niedermeier L, Chen K, Xing J, Das A, Kopsick J, Scott E, Sutton N, Weber K, Dutt N, Krichmar JL. 2022. CARLsim 6: An Open Source Library for Large-Scale, Biologically Detailed Spiking Neural Network Simulation2022 International Joint Conference on Neural Networks (IJCNN). Presented at the 2022 International Joint Conference on Neural Networks (IJCNN). Padua, Italy: IEEE. pp. 1–10. doi:10.1109/IJCNN55064.2022.9892644

Obafemi TO, Owolabi OV, Omiyale BO, Afolabi BA, Ojo OA, Onasanya A, Adu IAI, Rotimi D. 2021. Combination of donepezil and gallic acid improves antioxidant status and cholinesterases activity in aluminum chloride-induced neurotoxicity in Wistar rats. *Metabolic Brain Disease* **36**:2511–2519. doi:10.1007/s11011-021-00749-w

Petilla Interneuron Nomenclature Group, Ascoli GA, Alonso-Nanclares L, Anderson SA, Barrionuevo G, Benavides-Piccione R, Burkhalter A, Buzsáki G, Cauli B, Defelipe J, Fairén A, Feldmeyer D, Fishell G, Fregnac Y, Freund TF, Gardner D, Gardner EP, Goldberg JH, Helmstaedter M, Hestrin S, Karube F, Kisvárday ZF, Lambolez B, Lewis DA, Marin O, Markram H, Muñoz A, Packer A, Petersen CCH, Rockland KS, Rossier J, Rudy B, Somogyi P, Staiger JF, Tamas G, Thomson AM,

Toledo-Rodriguez M, Wang Y, West DC, Yuste R. 2008. Petilla terminology: nomenclature of features of GABAergic interneurons of the cerebral cortex. *Nature Reviews Neuroscience* **9**:557–568. doi:10.1038/nrn2402

Puighermanal E, Cutando L, Boubaker-Vitre J, Honoré E, Longueville S, Hervé D, Valjent E. 2017. Anatomical and molecular characterization of dopamine D1 receptor-expressing neurons of the mouse CA1 dorsal hippocampus. *Brain Structure & Function* **222**:1897–1911. doi:10.1007/s00429-016-1314-x

Rees CL, Moradi K, Ascoli GA. 2017. Weighing the Evidence in Peters' Rule: Does Neuronal Morphology Predict Connectivity?, Trends in Neurosciences. Elsevier Ltd. doi:10.1016/j.tins.2016.11.007

Rees CL, Wheeler DW, Hamilton DJ, White CM, Komendantov AO, Ascoli GA. 2016. Graph theoretic and motif analyses of the hippocampal neuron type potential connectome. *eNeuro* **3**. doi:10.1523/ENEURO.0205-16.2016

Ropireddy D, Scorcioni R, Lasher B, Buzsáki G, Ascoli GA. 2011. Axonal morphometry of hippocampal pyramidal neurons semi-automatically reconstructed after in vivo labeling in different CA3 locations. *Brain Structure & Function* **216**:1–15. doi:10.1007/s00429-010-0291-8

Sanchez-Aguilera A, Wheeler DW, Jurado-Parras T, Valero M, Nokia MS, Cid E, Fernandez-Lamo I, Sutton N, García-Rincón D, de la Prida LM, Ascoli GA. 2021. An update to Hippocampome.org by integrating single-cell phenotypes with circuit function in vivo. *PLoS Biology* **19**:e3001213. doi:10.1371/journal.pbio.3001213

Sáray S, Rössert CA, Appukuttan S, Migliore R, Vitale P, Lupascu CA, Bologna LL, Van Geit W, Romani A, Davison AP, Muller E, Freund TF, Káli S. 2021. HippoUnit: A software tool for the automated testing and systematic comparison of detailed models of hippocampal neurons based on electrophysiological data. *PLoS computational biology* **17**:e1008114. doi:10.1371/journal.pcbi.1008114

Sargolini F, Fyhn M, Hafting T, McNaughton BL, Witter MP, Moser M-B, Moser EI. 2006. Conjunctive representation of position, direction, and velocity in entorhinal cortex. *Science (New York, NY)* **312**:758–762. doi:10.1126/science.1125572

Savanthrapadian S, Meyer T, Elgueta C, Booker SA, Vida I, Bartos M. 2014. Synaptic properties of SOM- and CCK-expressing cells in dentate gyrus interneuron networks. *The Journal of Neuroscience: The Official Journal of the Society for Neuroscience* **34**:8197–8209. doi:10.1523/JNEUROSCI.5433-13.2014

Schumm SN, Gabrieli D, Meaney DF. 2022. Plasticity impairment exposes CA3 vulnerability in a hippocampal network model of mild traumatic brain injury. *Hippocampus* **32**:231–250. doi:10.1002/hipo.23402

Schumm SN, Gabrieli D, Meaney DF. 2020. Neuronal Degeneration Impairs Rhythms Between Connected Microcircuits. *Frontiers in Computational Neuroscience* **14**:18. doi:10.3389/fncom.2020.00018

Scorcioni R, Polavaram S, Ascoli GA. 2008. L-Measure: a web-accessible tool for the analysis, comparison and search of digital reconstructions of neuronal morphologies. *Nature Protocols* **3**:866–876. doi:10.1038/nprot.2008.51

Shepherd GM, Marenco L, Hines ML, Migliore M, McDougal RA, Carnevale NT, Newton AJH, Surles-Zeigler M, Ascoli GA. 2019. Neuron Names: A Gene- and Property-Based Name Format, With Special Reference to Cortical Neurons. *Frontiers in Neuroanatomy* **13**:25. doi:10.3389/fnana.2019.00025

Sik A, Tamamaki N, Freund TF. 1993. Complete axon arborization of a single CA3 pyramidal cell in the rat hippocampus, and its relationship with postsynaptic parvalbumin-containing interneurons. *The European journal of neuroscience* **5**:1719–28.

Skene NG, Grant SGN. 2016. Identification of Vulnerable Cell Types in Major Brain Disorders Using Single Cell Transcriptomes and Expression Weighted Cell Type Enrichment. *Frontiers in Neuroscience* **10**:16. doi:10.3389/fnins.2016.00016

Smith JH, Rowland C, Harland B, Moslehi S, Montgomery RD, Schobert K, Watterson WJ, Dalrymple-Alford J, Taylor RP. 2021. How neurons exploit fractal geometry to optimize their network connectivity. *Scientific Reports* **11**:2332. doi:10.1038/s41598-021-81421-2

Stein L, Sternberg P, Durbin R, Thierry-Mieg J, Spieth J. 2001. WormBase: network access to the genome and biology of Caenorhabditis elegans. *Nucleic Acids Research* **29**:82–86. doi:10.1093/nar/29.1.82

Steward O. 1976. Topographic organization of the projections from the entorhinal area to the hippocampal formation of the rat. *The Journal of Comparative Neurology* **167**:285–314. doi:10.1002/cne.901670303

Sutton NM, Ascoli GA. 2021. Spiking Neural Networks and Hippocampal Function: A Web-Accessible Survey of Simulations, Modeling Methods, and Underlying Theories. *Cognitive Systems Research* **70**:80–92. doi:10.1016/j.cogsys.2021.07.008

Takács VT, Klausberger T, Somogyi P, Freund TF, Gulyás AI. 2012. Extrinsic and local glutamatergic inputs of the rat hippocampal CA1 area differentially innervate pyramidal cells and interneurons. *Hippocampus* **22**:1379–1391. doi:10.1002/hipo.20974

Tecuatl C, Wheeler DW, Ascoli GA. 2021a. A Method for Estimating the Potential Synaptic Connections Between Axons and Dendrites From 2D Neuronal Images. *Bio-Protocol* **11**:e4073. doi:10.21769/BioProtoc.4073

Tecuatl C, Wheeler DW, Sutton N, Ascoli GA. 2021b. Comprehensive Estimates of Potential Synaptic Connections in Local Circuits of the Rodent Hippocampal Formation by Axonal-Dendritic Overlap. *The Journal of Neuroscience: The Official Journal of the Society for Neuroscience* **41**:1665–1683. doi:10.1523/JNEUROSCI.1193-20.2020

The FlyBase Consortium. 1994. FlyBase--the Drosophila database. *Nucleic Acids Research* **22**:3456–3458. doi:10.1093/nar/22.17.3456

Tsodyks M, Pawelzik K, Markram H. 1998. Neural networks with dynamic synapses. *Neural Computation* **10**:821–835. doi:10.1162/089976698300017502

Vaden RJ, Gonzalez JC, Tsai M-C, Niver AJ, Fusilier AR, Griffith CM, Kramer RH, Wadiche JI, Overstreet-Wadiche L. 2020. Parvalbumin interneurons provide spillover to newborn and mature dentate granule cells. *eLife* **9**:e54125. doi:10.7554/eLife.54125

Valero M, Cid E, Averkin RG, Aguilar J, Sanchez-Aguilera A, Viney TJ, Gomez-Dominguez D, Bellistri E, de la Prida LM. 2015. Determinants of different deep and superficial CA1 pyramidal cell dynamics during sharp-wave ripples. *Nature neuroscience* **18**:1281–1290. doi:10.1038/nn.4074

Venkadesh S, Komendantov AO, Listopad S, Scott EO, De Jong K, Krichmar JL, Ascoli GA. 2018. Evolving Simple Models of Diverse Intrinsic Dynamics in Hippocampal Neuron Types. *Frontiers in Neuroinformatics* **12**:8. doi:10.3389/fninf.2018.00008

Venkadesh S, Komendantov AO, Wheeler DW, Hamilton DJ, Ascoli GA. 2019. Simple models of quantitative firing phenotypes in hippocampal neurons: Comprehensive coverage of intrinsic diversity. *PLOS Computational Biology* **15**:e1007462. doi:10.1371/journal.pcbi.1007462

Venkadesh S, Van Horn JD. 2021. Integrative Models of Brain Structure and Dynamics: Concepts, Challenges, and Methods. *Frontiers in Neuroscience* **15**:752332. doi:10.3389/fnins.2021.752332

Walker AS, Raliski BK, Nguyen DV, Zhang P, Sanders K, Karbasi K, Miller EW. 2021. Imaging Voltage in Complete Neuronal Networks Within Patterned Microislands Reveals Preferential Wiring of Excitatory Hippocampal Neurons. *Frontiers in Neuroscience* **15**:643868. doi:10.3389/fnins.2021.643868

Wheeler DW, White CM, Rees CL, Komendantov AO, Hamilton DJ, Ascoli GA. 2015. Hippocampome.org: a knowledge base of neuron types in the rodent hippocampus. *eLife* **4**. doi:10.7554/eLife.09960

White CM, Rees CL, Wheeler DW, Hamilton DJ, Ascoli GA. 2020. Molecular expression profiles of morphologically defined hippocampal neuron types: Empirical evidence and relational inferences. *Hippocampus* **30**:472–487. doi:10.1002/hipo.23165

Winnubst J, Bas E, Ferreira TA, Wu Z, Economo MN, Edson P, Arthur BJ, Bruns C, Rokicki K, Schauder D, Olbris DJ, Murphy SD, Ackerman DG, Arshadi C, Baldwin P, Blake R, Elsayed A, Hasan M, Ramirez D, Dos Santos B, Weldon M, Zafar A, Dudman JT, Gerfen CR, Hantman AW, Korff W, Sternson SM, Spruston N, Svoboda K, Chandrashekar J. 2019. Reconstruction of 1,000 Projection Neurons Reveals New Cell Types and Organization of Long-Range Connectivity in the Mouse Brain. *Cell* **179**:268-281.e13. doi:10.1016/j.cell.2019.07.042

Winnubst J, Spruston N, Harris JA. 2020. Linking axon morphology to gene expression: a strategy for neuronal cell-type classification. *Current Opinion in Neurobiology* **65**:70–76. doi:10.1016/j.conb.2020.10.006

Wittner L, Henze DA, Záborszky L, Buzsáki G. 2007. Three-dimensional reconstruction of the axon arbor of a CA3 pyramidal cell recorded and filled in vivo. *Brain Structure & Function* **212**:75–83. doi:10.1007/s00429-007-0148-y

Wynne ME, Lane AR, Singleton KS, Zlatic SA, Gokhale A, Werner E, Duong D, Kwong JQ, Crocker AJ, Faundez V. 2021. Heterogeneous Expression of Nuclear Encoded Mitochondrial Genes Distinguishes Inhibitory and Excitatory Neurons. *eNeuro* **8**:ENEURO.0232-21.2021. doi:10.1523/ENEURO.0232-21.2021

Yao Z, Van Velthoven CTJ, Nguyen TN, Goldy J, Sedeno-Cortes AE, Baftizadeh F, Bertagnolli D, Casper T, Chiang M, Crichton K, Ding S-L, Fong O, Garren E, Glandon A, Gouwens NW, Gray J, Graybuck LT, Hawrylycz MJ, Hirschstein D, Kroll M, Lathia K, Lee C, Levi B, McMillen D, Mok S, Pham T, Ren Q, Rimorin C, Shapovalova N, Sulc J, Sunkin SM, Tieu M, Torkelson A, Tung H, Ward K, Dee N, Smith KA, Tasic B, Zeng H. 2021. A taxonomy of transcriptomic cell types across the isocortex and hippocampal formation. *Cell* **184**:3222-3241.e26. doi:10.1016/j.cell.2021.04.021

Yeung AWK, Goto TK, Leung WK. 2017. The Changing Landscape of Neuroscience Research, 2006-2015: A Bibliometric Study. *Frontiers in Neuroscience* **11**:120. doi:10.3389/fnins.2017.00120

Yuste R, Hawrylycz M, Aalling N, Aguilar-Valles A, Arendt D, Armañanzas R, Ascoli GA, Bielza C, Bokharaie V, Bergmann TB, Bystron I, Capogna M, Chang Y, Clemens A, de Kock CPJ, DeFelipe J, Dos Santos SE, Dunville K, Feldmeyer D, Fiáth R, Fishell GJ, Foggetti A, Gao X, Ghaderi P, Goriounova NA, Güntürkün O, Hagihara K, Hall VJ, Helmstaedter M, Herculano-Houzel S, Hilscher MM, Hirase H, Hjerling-Leffler J, Hodge R, Huang J, Huda R, Khodosevich K, Kiehn O, Koch H, Kuebler ES, Kühnemund M, Larrañaga P, Lelieveldt B, Louth EL, Lui JH, Mansvelder HD, Marin O, Martinez-Trujillo J, Chameh HM, Mohapatra AN, Munguba H, Nedergaard M, Němec P, Ofer N, Pfisterer UG, Pontes S, Redmond W, Rossier J, Sanes JR, Scheuermann RH, Serrano-Saiz E, Staiger JF, Somogyi P, Tamás G, Tolias AS, Tosches MA, García MT, Wozny C, Wuttke TV, Liu Y, Yuan J, Zeng H, Lein E. 2020. A community-based transcriptomics classification and nomenclature of neocortical cell types. *Nature Neuroscience* **23**:1456–1468. doi:10.1038/s41593-020-0685-8

Zagrean A-M, Georgescu I-A, Iesanu MI, Ionescu R-B, Haret RM, Panaitescu AM, Zagrean L. 2022. Oxytocin and vasopressin in the hippocampus. *Vitamins and Hormones* **118**:83–127. doi:10.1016/bs.vh.2021.11.002

Zeisel A, Moz-Manchado AB, Codeluppi S, Lönnerberg P, Manno GL, Juréus A, Marques S, Munguba H, He L, Betsholtz C, Rolny C, Castelo-Branco G, Hjerling-Leffler J, Linnarsson S. 2015. Cell types in the mouse cortex and hippocampus revealed by single-cell RNA-seq. *Science* **347**:1138–1142. doi:10.1126/science.aaa1934

973 Zeng H, Sanes JR. 2017. Neuronal cell-type classification: challenges, opportunities and the path
974 forward. *Nature Reviews Neuroscience* **18**:530–546. doi:10.1038/nrn.2017.85
975
976

977 **Tables**

978

979 **Table 1. Added knowledge and functioning in Hippocampome.org releases v1.1-12.**

980

Version	Contribution	Article
v1.1	• definitions for terms and phrases relevant to Hippocampome.org	(Hamilton et al., 2017a)
v1.2	• clickable connectivity matrix • interactive connectivity navigator Java applet • searching by connectivity	(Rees et al., 2016)
v1.3	• downloadable list of ABA predictions of marker expressions • utility for viewing the effects of thresholds on ABA marker expression predictions	(Hamilton et al., 2017b)
v1.4	• access to the synapse knowledge base	(Moradi and Ascoli, 2020)
v1.5	• relational biomarker expression inferences	(White et al., 2020)
v1.6	• firing pattern phenotypes • clickable firing pattern matrix • clickable firing pattern parameters matrix • search by firing pattern • search by firing pattern parameter	(Komendantov et al., 2019)
v1.7	• Izhikevich models • clickable Izhikevich model parameters matrix • downloadable single-neuron parameter files • downloadable single-neuron CARLSim4 simulation files • ability to perform single-neuron simulations of the firing patterns	(Venkadesh et al., 2019)
v1.8	• clickable/downloadable neurite lengths matrix • clickable/downloadable somatic path distances matrix • clickable/downloadable numbers of potential synapses matrix • clickable/downloadable numbers of contacts matrix • clickable/downloadable connection probabilities matrix	(Tecuatl et al., 2021b)
v1.9	• clickable matrix for in vivo recordings	(Sanchez-Aguilera et al., 2021)
v1.10	• Cognome knowledge base of spiking neural circuit functions and network simulations of the hippocampal formation	(Sutton and Ascoli, 2021)
v1.11	• clickable matrix of neuron type census values for rat and mouse	(Attili et al., 2022)
v1.12	• clickable/downloadable matrices of synaptic physiology parameter values (g, τ_d, τ_r, τ_f, U) for combinations of species, sex, age, temperature, and recording mode	(Moradi et al., 2022)

981

982 **Table 2.** Probabilities of connection and number of contacts per connected pair from DG
983 Granule cell to mossy fibers targets in CA3.
984

Postsynaptic neuron type	Probability	# contacts
CA3 Pyramidal	5.10E-05	1.07
CA3c Pyramidal	1.68E-04	1.25
CA3 Spiny Lucidum Dentate-Projecting	5.89E-04	1.69
CA3 Mossy Fiber-Associated ORDEN	1.92E-04	1.26
CA3 Basket	1.19E-04	1.10
CA3 Basket CCK+	9.28E-05	1.11
CA3 Ivy	1.04E-04	1.16
CA3 Mossy Fiber-Associated	1.90E-04	1.28
CA3 LMR-Targeting	1.31E-04	1.21
CA3 Lucidum ORAX	2.62E-04	1.19
CA3 Lucidum-Radiatum	3.25E-04	1.13
CA3 Axo-Axonic	4.68E-05	1.06
CA3 Bistratified	3.31E-04	1.38
CA3 QuadD-LM	2.96E-04	1.29

985
986

987 **Table 3. Examples of independent studies utilizing unique neuronal properties from**
988 **Hippocampome.org v1.0.**
989

Article	Usage
(Gulyás et al., 2016)	Lists of subthreshold physiological properties for multicompartmental modeling
(Skene and Grant, 2016)	Catalog of CA1 Interneuron types
(Faghihi and Moustafa, 2017)	Diversity of hippocampal neuron types and morphological neuronal features
(Puighermanal et al., 2017)	Biomarker expression in CA1 interneurons
(Depannemaecker et al., 2020)	Parameter values for a model of synaptic neurotransmission
(Ecker et al., 2020)	Evidence that CA1 interneurons express multiple overlapping chemical markers
(Hunsberger and Mynlieff, 2020)	Cell identification based on firing properties
(Schumm et al., 2020)	Directionality of connections in the hippocampus
(Aery Jones et al., 2021)	Local connectivity of CA1 PV+ interneurons
(Ciarpella et al., 2021)	Lists of hippocampal genes
(Luo et al., 2021)	Confirmation of multiple hippocampal neuron types
(Mehta et al., 2021)	Connectome model inspired by entorhinal-CA1 circuit
(Obafemi et al., 2021)	Principal channels of information processing are DG Granule cells and CA1-3 Pyramidal cells
(Sáray et al., 2021)	Membrane biophysics values for CA1 Pyramidal cells
(Smith et al., 2021)	Omni-directionality of axons of CA1 Pyramidal cells
(Venkadesh and Van Horn, 2021)	Example of a brain region's mesoscopic structural connectivity
(Walker et al., 2021)	Reference to morphological and molecular characteristics of hippocampal principal cells and interneurons
(Wynne et al., 2021)	Example brain region with a variety of cell types
(Kopsick et al., 2022)	Utilize accumulated knowledge as the basis for simulations
(Schumm et al., 2022)	Hippocampal morphology, biomarker expression, connectivity, and typing of neurons
(Zagrean et al., 2022)	Diversity of hippocampal neuronal types and their properties

990

991 **Figure Legends**
992
993 **Figure 1.** Defining neuron types in Hippocampome.org. A) Properties of a Hippocampome.org v1.0
994 neuron type. A1) Morphology of a DG (i)2232 Basket cell (NeuroMorpho.Org cell NMO_34300: Hosp et
995 al., 2014) with axons (red) in SG and dendrites (blue) in all four layers. A2) Schematic interpretation of
996 the morphological tracing, where the circle represents the location of the soma in SG, the red triangle
997 the location of the axons in SG, and the blue rectangles the locations of the dendrites in all four layers.
998 A3) Hippocampome.org representation of the morphology, where a blue square with a vertical line (|)
999 indicates dendritic presence in SMo and SMi and H, a purple square with a cross (+) indicates both
1000 axonal and dendritic presence in SG, and a black dot (•) indicates the soma location in SG. A4)
1001 Hippocampome.org numerical coding of the reconstructed neuron, where 2 indicates the presence of
1002 dendrites (in SMo, SMi, and H); and 3 indicates the presence of both axons and dendrites (in SG). A5)
1003 Biomarker expressions, where a green triangle indicates positive expression, and a blue triangle
1004 indicates negative expression. A6) Firing pattern phenotype (NASP; adapted from Figure 1B1 in
1005 Savanthrapadian et al., 2014). A7) Membrane biophysics values (from Figure 3C and Table 1 in Lübke et
1006 al., 1998) recorded at 35-37 °C. B) Properties for a Hippocampome.org v2.0 neuron type. B1)
1007 Morphology of a DG (i)2210 Basket GRALDEN (NeuroMorpho.Org cell NMO_146159: Vaden et al., 2020)
1008 with red axons in SG and blue dendrites in SMo and SMi. B2) Schematic interpretation of the
1009 reconstruction (same symbols as in A2). B3-4) Hippocampome.org representation and numerical coding
1010 of the morphology (same symbols as in A3-4). B5) Biomarker expression. B6) Firing pattern phenotype
1011 (TSTUT.SLN; adapted from Figure S4 in Markwardt et al., 2011). B7) Membrane biophysics values
1012 recorded at room temperature (from Figure 4D in Vaden et al., 2020), and at 22 °C (from Figure S4 in
1013 Markwardt et al., 2011); emboldened values were extracted from the firing pattern trace in B6.
1014 Abbreviations are defined in Materials and Methods.
1015
1016 **Figure 2.** New neuron types added to Hippocampome.org v2.0. A) Morphology encodings of the 51 new
1017 neuron types. (Left) Increase in number of neuron types for each subregion. B) Biomarker expressions of
1018 the neuron types. C) Membrane biophysics values for the neuron types. Abbreviations are defined in
1019 Materials and Methods.
1020
1021 **Figure 3.** Extensions to the neuronal properties of Hippocampome.org v1.x. A1) Additions to the axonal
1022 projections (circled in green) for two v1.0 neuron types. A2) Evidence for the axonal extensions in strata
1023 oriens, pyramidale, and radiatum from A1 are circled in green (adapted from Figure 2b in Deller et al.,
1024 1996). Scale bar: 75 µm. B1) Biomarker expressions for the two CA1 Pyramidal sub-types added in
1025 Hippocampome.org v1.9 (Sanchez-Aguilera et al., 2021). B2) Membrane biophysics values for the two
1026 sub-types. B3) CA2 projects preferentially to the deep sublayer of CA1 (Kohara et al., 2014). More
1027 perisomatic PV+ GABAergic boutons are found at CA1 Deep Pyramidal cells (Valero et al., 2015). CA1
1028 Superficial Pyramidal cells form more frequent connections to PV+ CA1 Basket cells, and PV+ CA1 Basket
1029 cells form significantly more perisomatic axon terminals on CA1 Deep Pyramidal cells (Lee et al., 2014).
1030 C1) Additions to the firing pattern phenotypes of v1.0 neuron types. C2a) Example of ASP. in a CA3
1031 Basket cell (adapted from Figure 2d in Fidzinski et al., 2015). C2b) Example of NASP in a CA3 Bistratified
1032 cell (adapted from Figure 2e in Fidzinski et al., 2015). C2c) Example of TSTUT. in a CA1 Radiatum Giant
1033 cell (adapted from Figure 2Bb in Kirson and Yaari, 2000). C2d) Example of TSTUT.SLN in a DG MOLAX cell
1034 (adapted from Figure S2c in Lee et al., 2016). C2e) Example of TSTUT.PSTUT in a CA1 Interneuron
1035 Specific O-targeting QuadD (adapted from Figure 2D in Chamberland et al., 2010). D) Synaptic
1036 probabilities for projecting connections and the corresponding number of contacts in brackets between

the two CA3 Pyramidal neuron types and a selection of CA1 neuron types. Abbreviations are defined in Materials and Methods.

Figure 4. Trends in Hippocampome.org data, knowledge, citations, and usage since v1.0. A) Increase in pieces of knowledge (blue) and evidence (red) with Hippocampome.org version number. B) Number of citations, in which the publication is simply referenced (blue and gray portions), and usage cases, in which the citing work makes use of the information contained within the Hippocampome.org-related work (orange and yellow portions), by year.

Figure 5. Transitional knowledge enabling Hippocampome.org to support spiking neural network simulations. Center: General diagram of the hippocampal formation and the number of cell types in Hippocampome v1.0. A) Neuron type census. Top: General pipeline for obtaining cell counts for specific collections of neurons from the peer reviewed literature. Left: Neuron count proportions for the different subregions of the hippocampal formation. Insert: Normalized neuron counts for the inhibitory vs. excitatory balance by subregion. Right: Neuron counts for five identified CA2 neuron types (green schematic: excitatory, red schematic: inhibitory). B) Neuron dynamics. Top: General pipeline for obtaining Izhikevich models to reproduce the firing pattern phenotypes from peer reviewed data. Right: Simulated firing pattern from a Sub CA1-Projecting Pyramidal cell in response to a 250-pA current injection pulse lasting 1 s. Izhikevich model parameters are shown in bold and the membrane biophysics properties are shown in regular font. C) Synaptic probabilities. Left: General pipeline for obtaining the connection probabilities, number of contacts, and dendritic and axonal path lengths from 2D reconstructions. Middle: Example of a connectivity diagram of a DG Granule cell and two interneurons across the different parcels of DG. Probabilities of connection (mean ± SD) are shown in black, numbers of contacts in gray, dendritic path lengths in blue, and axonal lengths in red. Right top: Total number of connections within DG by connection type. Right bottom: Breakdown of the total number of connections by parcel and connection type. D) Synaptic physiology. Left: General pipeline for obtaining normalized synaptic parameters from paired recordings with a TPM model. Right top: Digitized synaptic data between two EC LII-III Pyramidal-Tripolar cells. Experimental data are shown in blue, initiation synaptic points in pink, model data in orange, and corrected data in green. Right bottom: Simulated modeling conditions, electrophysiological parameters, and TPM parameters. Abbreviations are defined in Materials and Methods.

Figure 6. Hippocampome.org data provenance. A) The internal web of constituent neuron-type properties (thin arrows) that ultimately contribute to the instantiation of spiking neural simulations (thick arrows). Properties described qualitatively, such as morphological presence of axons in a layer or molecular biomarker expressions, are in black font. Properties described by quantitative values, such as membrane biophysics and neurite lengths, are in red font. Properties with v2.0 updated information, such as connectivity and firing pattern phenotypes, are depicted by blue hexagons, and v1.x information, such as Izhikevich modeling parameter values and neuron-type census values, is visualized by black circles. B) External resources that contribute data to and receive data from Hippocampome.org (the ModelDB logo has been modified from the original).

Figure 7. CARLsim simulation parameters selection and file generation interface. A) The user chooses which subset of the available neuron types to include in the generated downloadable parameter file. Neuron types can be selected (check boxes and gray highlights) either individually or by groupings, such as by subregion and/or by importance rank. B) Representative user selection. C) Downloadable neuron-level parameters. D) Downloadable connection-level parameters.

1085 **Figure 8.** Hierarchy of neuronal connectivity in Hippocampome.org. A) Subregional connectivity, where
1086 the number of connections between subregions is shown, and the node size is proportional to the
1087 number of neuron types in each subregion. B) The reciprocal connectivity between DG and CA3 neuron
1088 types consists of 147 connections. The node size is proportional to the census size for each neuron type.
1089 C) The full connectivity involving DG Granule and CA3 Basket neuron types consists of 98 connections.
1090 The node size is proportional to the census size for each neuron type, and the thicknesses of the
1091 connecting arrows are proportional to the synaptic probability. The dashed lines are connections for
1092 which the synaptic probability has been approximated based on the means of known values. D) The
1093 electrophysiological connection between a DG Granule cell and a CA3 Basket cell. The in vivo firing rate
1094 is shown for the presynaptic neuron. The transfer function between the two neuron types is
1095 proportional to the synaptic conductance times the single-exponential decay time constant ($g \cdot \tau_d$; rat,
1096 male, P56, 32°C, current clamp). The frequency-current (F-I) curve of the single-compartment Izhikevich
1097 model of a CA3 Basket cell was obtained with 10 pA current steps. Inset: Izhikevich model firing pattern
1098 of a CA3 Basket cell simulated with 430 pA of current applied for 500 ms (vertical and horizontal scale
1099 bars, respectively).
1100
1101 **Figure 9.** Spiking neural network simulations. A) Full-scale CA3 model. (Aa) Neuron type connectivity
1102 schematic. (Ab) Theta (4-12 Hz; top), Gamma (25-100 Hz; middle), and Sharp-Wave Ripple (150-200 Hz;
1103 bottom) filtered local field potentials from 175 ms of the simulation. (Ac) Raster plot of 500 Pyramidal
1104 cells and 50 interneurons of each type (top), and representative voltage traces for each neuron type
1105 during the same 175 ms of the simulation in (Ab). B) Spatial representation through grid cell firing. (Ba)
1106 Neuron type connectivity schematic. Bb) Simulated animal trajectory (black) with red dots indicating the
1107 firing of a neuron in those locations. Bc) Raster plot of 50 randomly selected neurons from each type
1108 (top), and representative voltage traces for each neuron type. Abbreviations are defined in Materials
1109 and Methods.

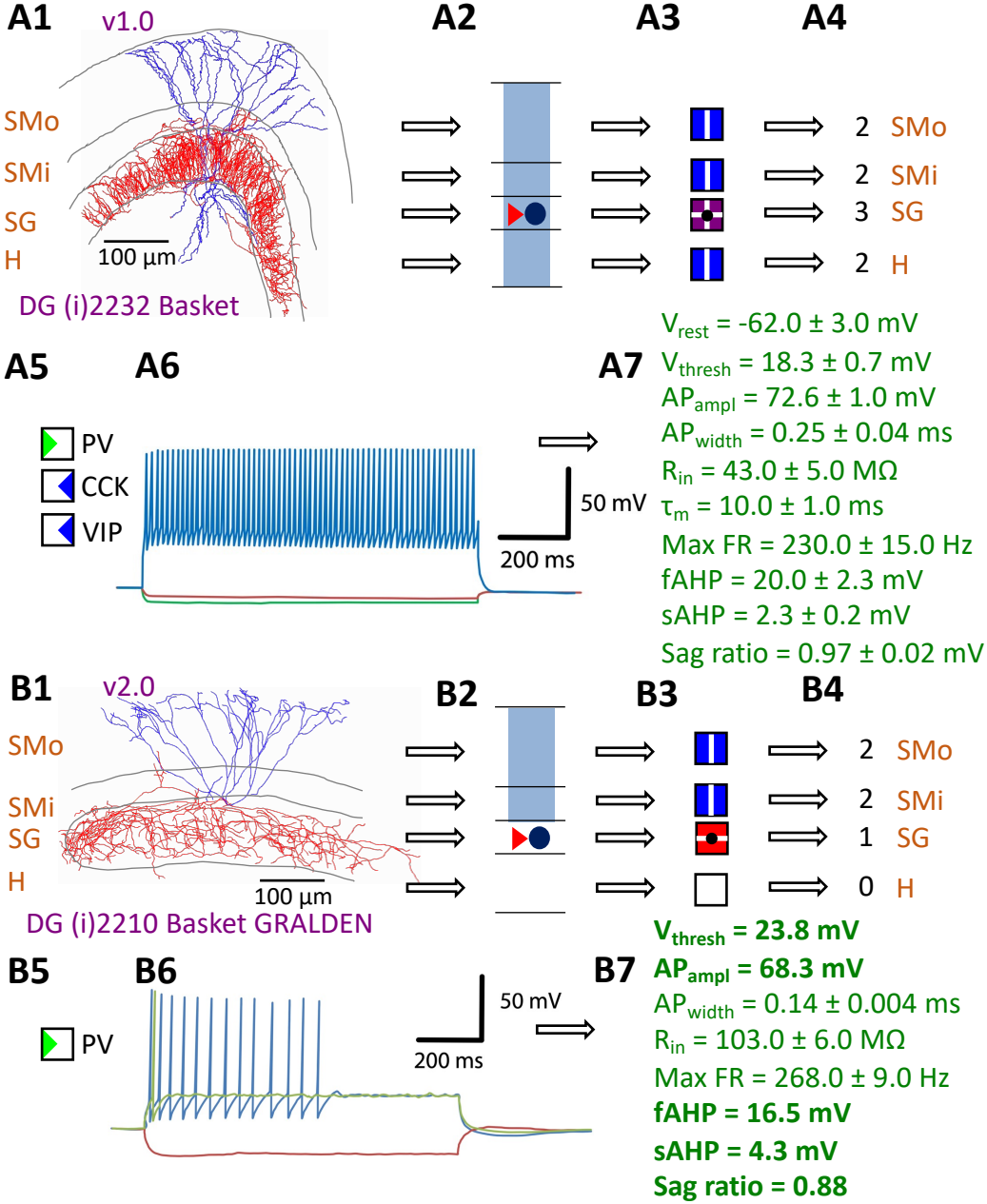
A1
v1.0
SMo
SMi
SG
H
100 µm
DG (i)2232 Basket
A2
A3
A4
2 SMo
2 SMi
3 SG
2 H
A5
A6
A7
PV
CCK
VIP
50 mV
200 ms
V_{rest} = -62.0 ± 3.0 mV
V_{thresh} = 18.3 ± 0.7 mV
AP_{ampl} = 72.6 ± 1.0 mV
AP_{width} = 0.25 ± 0.04 ms
R_{in} = 43.0 ± 5.0 MΩ
τ_m = 10.0 ± 1.0 ms
Max FR = 230.0 ± 15.0 Hz
fAHP = 20.0 ± 2.3 mV
sAHP = 2.3 ± 0.2 mV
Sag ratio = 0.97 ± 0.02 mV
B1
v2.0
SMo
SMi
SG
H
100 µm
DG (i)2210 Basket GRALDEN
B2
B3
B4
2 SMo
2 SMi
1 SG
0 H
B5
B6
B7
PV
50 mV
200 ms
V_{thresh} = 23.8 mV
AP_{ampl} = 68.3 mV
AP_{width} = 0.14 ± 0.004 ms
R_{in} = 103.0 ± 6.0 MΩ
Max FR = 268.0 ± 9.0 Hz
fAHP = 16.5 mV
sAHP = 4.3 mV
Sag ratio = 0.88

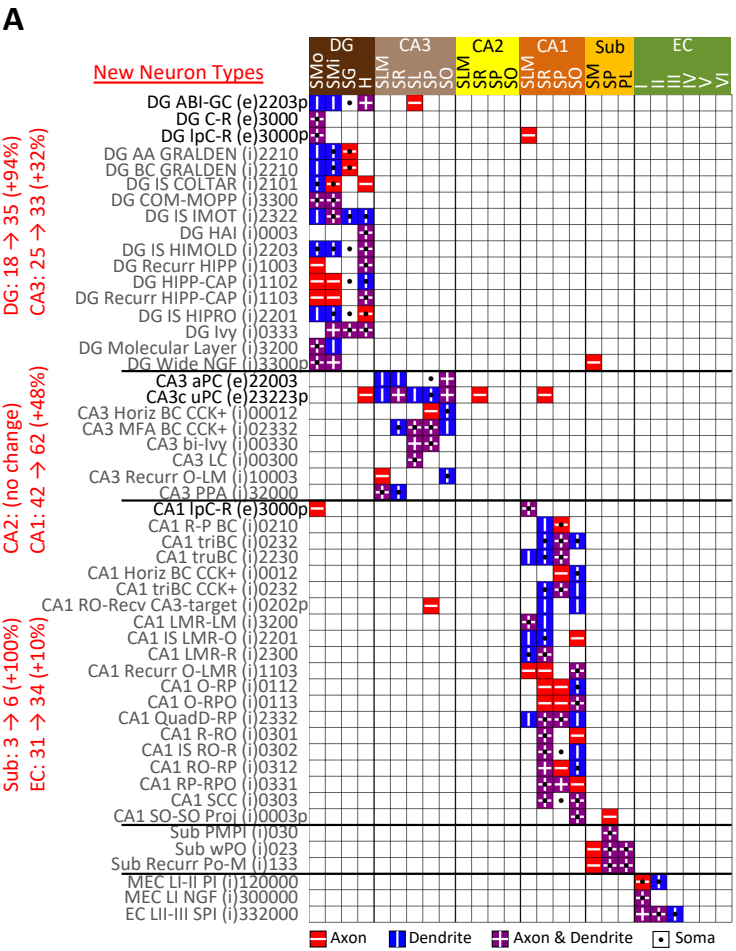

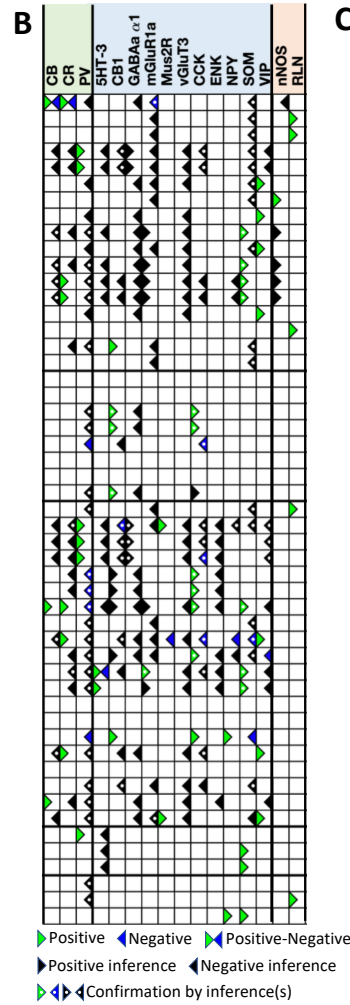

C

V_{rest} (mV)	R_{in} (MΩ)	τ_m (ms)	V_{threh} (mV)	Fast AHP (mV)	AP_{ampl} (mV)	AP_{width} (ms)	Max FR (Hz)
-45.6	2.9	67.4		6.1	43.8		
	103.0					0.14	268.0
-60.8	812.0		22.9		75.7	0.91	30.3
-87.7	171.1	7.1		17.7	72.8		70.0
-49.3	1089.0		12.0	19.4	82.9	1.04	12.2
-57.1	186.7	9.3				0.62	141.5
-47.5	889.0		11.3		71.6	0.88	25.2
-61.0	59.0	9.0		14.7	56.0	1.50	
	295.0	40.8				1.90	
	176.9					0.65	
-47.5	889.0		11.3		71.6	0.88	25.2
	354.0	21.6		16.1	54.7	1.50	
-63.0	292.0	10.9		17.7	72.8	1.10	108.0
-68.5	124.6		18.2	2.0	76.8		
-62.0	52.0	16.0			67.4	2.74	
	0.8	0.8		0.8		0.77	
-59.0	341.0	42.0		15.1		0.80	75.0
	198.0	22.0		13.7		1.30	41.3
-59.2	114.8					0.40	108.8
-63.6	251.4	12.5	20.3		80.4	1.02	156.0
-62.9	76.4				81.1	0.23	
	174.0	40.8		1.4		0.80	47.0
-57.7	32.1		13.7	18.4	63.9		
	507.0	92.8					
-74.2	496.9	19.1	29.6		86.3	1.10	171.0
	220.0	42.6				1.10	52.0
-65.0	306.0	38.0	24.0	17.6	64.0		
-63.4	204.2				87.1	0.43	62.2
	342.0	28.0				1.55	
	220.0	42.6				1.10	52.0
	600.0	60.0					
	738.0	76.0					
-59.5	196.4		16.8	14.6	65.3	0.70	
-67.0	137.0			23.0	64.0	0.34	
-49.9	387.8				91.8	1.50	26.0
-49.9	387.8				91.8	1.50	26.0
	148.9			17.6		0.42	85.0
-65.1		7.5					
-74.1	385.0	34.6	22.1		77.4	0.93	

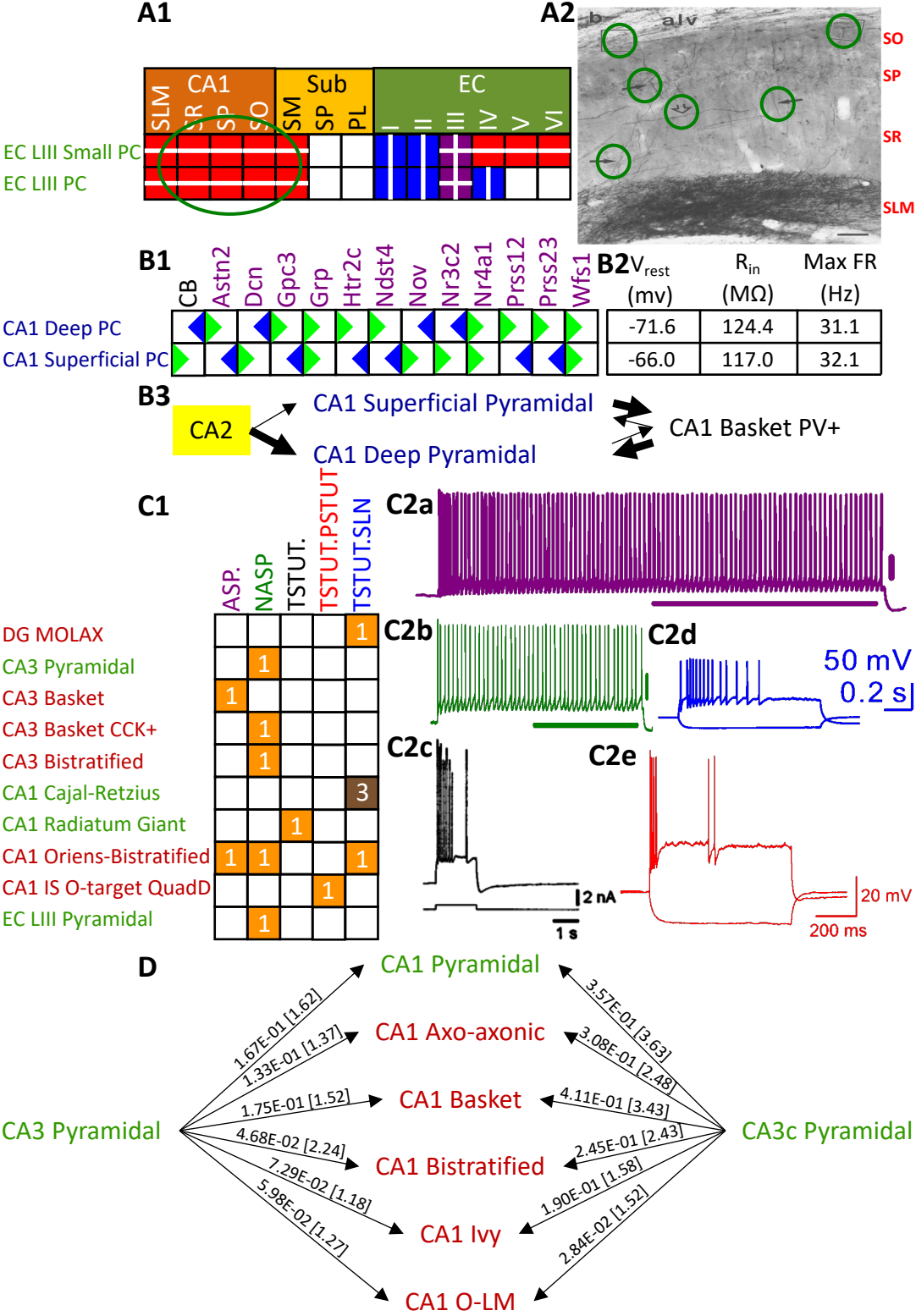
A1
CA1
SLM
SR
SP
SO
Sub
SM
SP
PL
EC
I
II
III
IV
V
VI
EC LIII Small PC
EC LIII PC
A2
alv
SO
SP
SR
SLM
B1
CB
Astn2
Dcn
Gpc3
Grp
Htr2c
Ndst4
Nov
Nr3c2
Nr4a1
Prss12
Prss23
Wfs1
CA1 Deep PC
CA1 Superficial PC
B2
V_{rest} (mv)
R_{in} (MΩ)
Max FR (Hz)
-71.6 124.4 31.1
-66.0 117.0 32.1
B3
CA2
CA1 Superficial Pyramidal
CA1 Deep Pyramidal
CA1 Basket PV+
C1
ASP.
NASP
TSTUT.
TSTUT.PSTUT
TSTUT.SLN
DG MOLAX
CA3 Pyramidal
CA3 Basket
CA3 Basket CCK+
CA3 Bistratified
CA1 Cajal-Retzius
CA1 Radiatum Giant
CA1 Oriens-Bistratified
CA1 IS O-target QuadD
EC LIII Pyramidal
C2a
C2b
C2c
C2d
C2e
50 mV
0.2 s
2 nA
1 s
20 mV
200 ms
D
CA1 Pyramidal
CA1 Axo-axonic
CA1 Basket
CA1 Bistratified
CA1 Ivy
CA1 O-LM
CA3 Pyramidal
CA3c Pyramidal
1.67E-01 [1.62]
1.33E-01 [1.37]
1.75E-01 [1.52]
4.68E-02 [2.24]
7.29E-02 [1.18]
5.98E-02 [1.27]
3.57E-01 [3.63]
3.08E-01 [2.48]
4.11E-01 [3.43]
2.45E-01 [2.43]
1.90E-01 [1.58]
2.84E-02 [1.52]

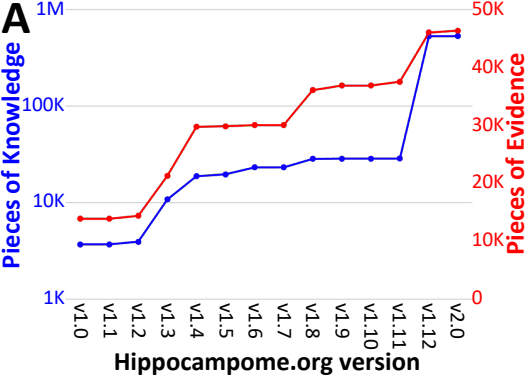
A
Pieces of Knowledge
1M
100K
10K
1K
Pieces of Evidence
50K
40K
30K
20K
10K
0
v1.0
v1.1
v1.2
v1.3
v1.4
v1.5
v1.6
v1.7
v1.8
v1.9
v1.10
v1.11
v1.12
v2.0
Hippocampome.org version

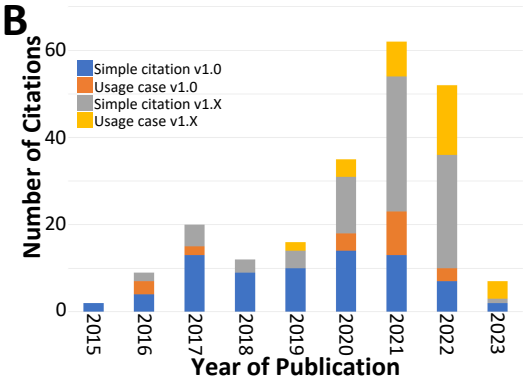
B
Number of Citations
60
40
20
0
Simple citation v1.0
Usage case v1.0
Simple citation v1.X
Usage case v1.X
2015
2016
2017
2018
2019
2020
2021
2022
2023
Year of Publication

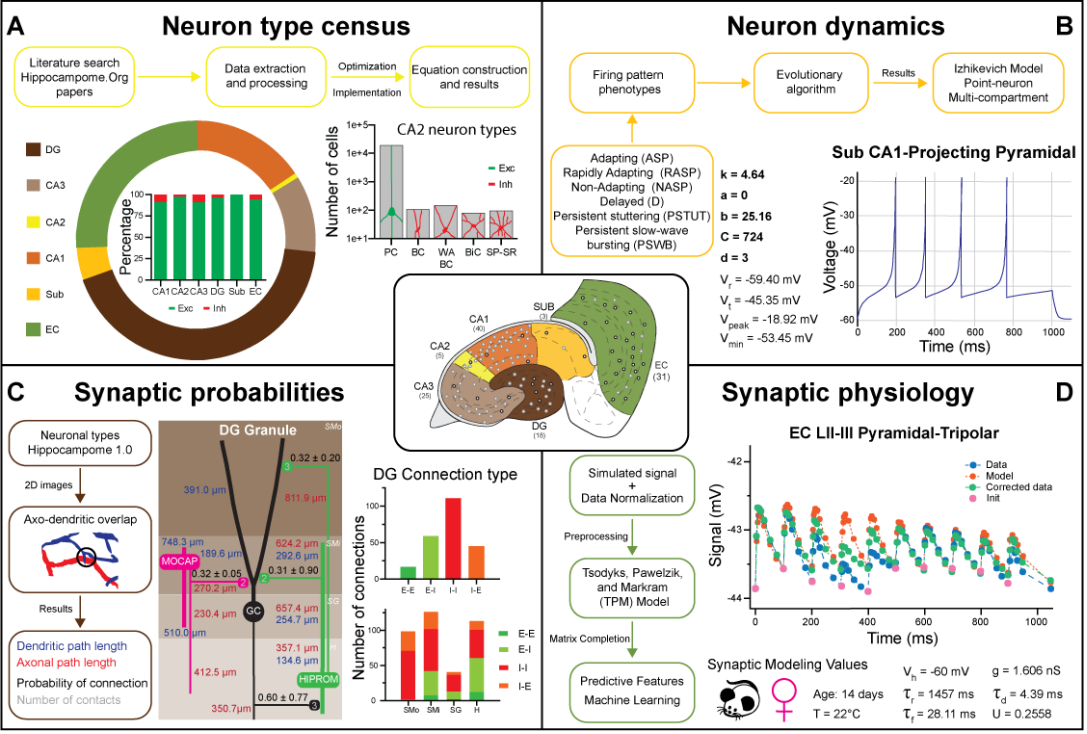
A
Neuron type census
Literature search Hippocampome.Org papers
Data extraction and processing
Optimization
Implementation
Equation construction and results
DG
CA3
CA2
CA1
Sub
EC
Percentage
CA1 CA2 CA3 DG Sub EC
Exc
Inh
CA2 neuron types
Number of cells
PC BC WA BC BiC SP-SR
B
Neuron dynamics
Firing pattern phenotypes
Evolutionary algorithm
Results
Izhikevich Model Point-neuron Multi-compartment
Adapting (ASP)
Rapidly Adapting (RASP)
Non-Adapting (NASP)
Delayed (D)
Persistent stuttering (PSTUT)
Persistent slow-wave bursting (PSWB)
k = 4.64
a = 0
b = 25.16
C = 724
d = 3
V_r = -59.40 mV
V_t = -45.35 mV
V_peak = -18.92 mV
V_min = -53.45 mV
Sub CA1-Projecting Pyramidal
Voltage (mV)
Time (ms)
CA1 (40)
SUB (3)
CA2 (5)
CA3 (25)
DG (18)
EC (31)
C
Synaptic probabilities
Neuronal types Hippocampome 1.0
2D images
Axo-dendritic overlap
Results
Dendritic path length
Axonal path length
Probability of connection
Number of contacts
DG Granule
SMo
SMi
SG
H
MOCAP
HIPROM
GC
391.0 µm
811.9 µm
748.3 µm
189.6 µm
624.2 µm
292.6 µm
0.32 ± 0.20
0.32 ± 0.05
0.31 ± 0.90
270.2 µm
230.4 µm
657.4 µm
254.7 µm
510.0 µm
357.1 µm
134.6 µm
412.5 µm
0.60 ± 0.77
350.7µm
DG Connection type
Number of connections
E-E
E-I
I-I
I-E
SMo SMi SG H
D
Synaptic physiology
Simulated signal + Data Normalization
Preprocessing
Tsodyks, Pawelzik, and Markram (TPM) Model
Matrix Completion
Predictive Features Machine Learning
EC LII-III Pyramidal-Tripolar
Data
Model
Corrected data
Init
Signal (mV)
Time (ms)
Synaptic Modeling Values
Age: 14 days
T = 22°C
V_h = -60 mV
g = 1.606 nS
τ_r = 1457 ms
τ_d = 4.39 ms
τ_f = 28.11 ms
U = 0.2558

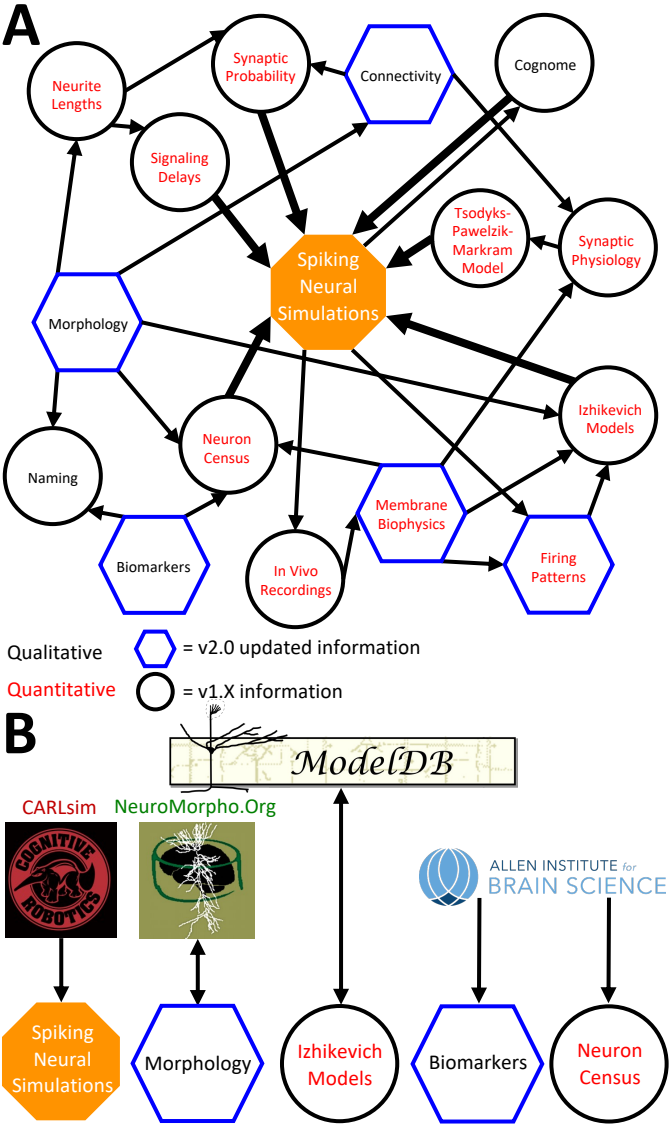
A
Neurite Lengths
Synaptic Probability
Connectivity
Cognome
Signaling Delays
Tsodyks-Pawelzik-Markram Model
Synaptic Physiology
Spiking Neural Simulations
Morphology
Izhikevich Models
Neuron Census
Naming
Membrane Biophysics
Biomarkers
In Vivo Recordings
Firing Patterns
Qualitative
= v2.0 updated information
Quantitative
= v1.X information
B
ModelDB
CARLsim
NeuroMorpho.Org
ALLEN INSTITUTE for BRAIN SCIENCE
Spiking Neural Simulations
Morphology
Izhikevich Models
Biomarkers
Neuron Census

A

Hippocampome.org

Simulation Parameters Selection

Download a precomputed parameter set zip file:

DG CA3 CA2 CA1

Sub EC All

OR select a user-defined parameter set:

☐ All neuron types

Generate zip file

☐ DG ☐ CA3 ☐ CA2 ☐ CA1 ☐ Sub ☐ EC

☐ All rank 1-5 neuron types

☐ All rank 1-3 neuron types

☐ All canonical neuron types

B

DG (0/35)	CA3 (0/33)	CA2 (3/5)
☐ DG Granule	☐ CA3 Pyramidal	☐ CA2 Pyramidal
☐ DG Semilunar GC	☐ CA3c Pyramidal	☐ CA2 Basket
☐ DG Mossy	☐ CA3 Giant	☐ CA2 Wide-Arbor BC
☐ DG AIPRIM	☐ CA3 Granule	☐ CA2 Bistratified
☐ DG Axo-axonic	☐ CA3 Axo-axonic	☐ CA2 SP-SR

C

Neuron Type	E/I	rank	Population Size	Izh Vr	Izh Vt	Izh a	Izh b	Izh k	Izh d	Izh C
CA2_Pyramidal	e	3	18956	-72.59	-58.78	0.00	-15.89	5.94	74	1630
CA2_Basket	i	3	105	-70.31	-49.91	0.01	-28.48	5.12	132	150
CA2_Bistratified	i	3	79	-74.10	-40.19	0.01	4.75	0.80	4	118

D

Presynaptic	Postsynaptic	TPM g	TPM tau_d	TPM tau_r	TPM tau_f	TPM U	Conn Prob
CA2_Pyramidal	CA2_Pyramidal	2.54	3.42	215.28	102.02	0.29	0.03091
CA2_Basket	CA2_ Pyramidal	3.98	6.25	580.69	10.61	0.27	0.01000
CA2_Bistratified	CA2_ Pyramidal	4.58	5.70	588.65	10.00	0.28	0.08168
CA2_Pyramidal	CA2_ Basket	4.44	2.46	138.68	163.55	0.37	0.03159
CA2_Basket	CA2_Basket	2.78	5.41	508.31	28.25	0.26	0.01000
CA2_Bistratified	CA2_ Basket	3.16	4.93	510.18	27.01	0.26	0.08287
CA2_Pyramidal	CA2_ Bistratified	2.32	2.47	143.16	122.67	0.29	0.04682
CA2_Basket	CA2_ Bistratified	2.06	5.59	504.11	22.74	0.24	0.01000
CA2_Bistratified	CA2_Bistratified	2.29	5.12	508.27	21.67	0.24	0.09951

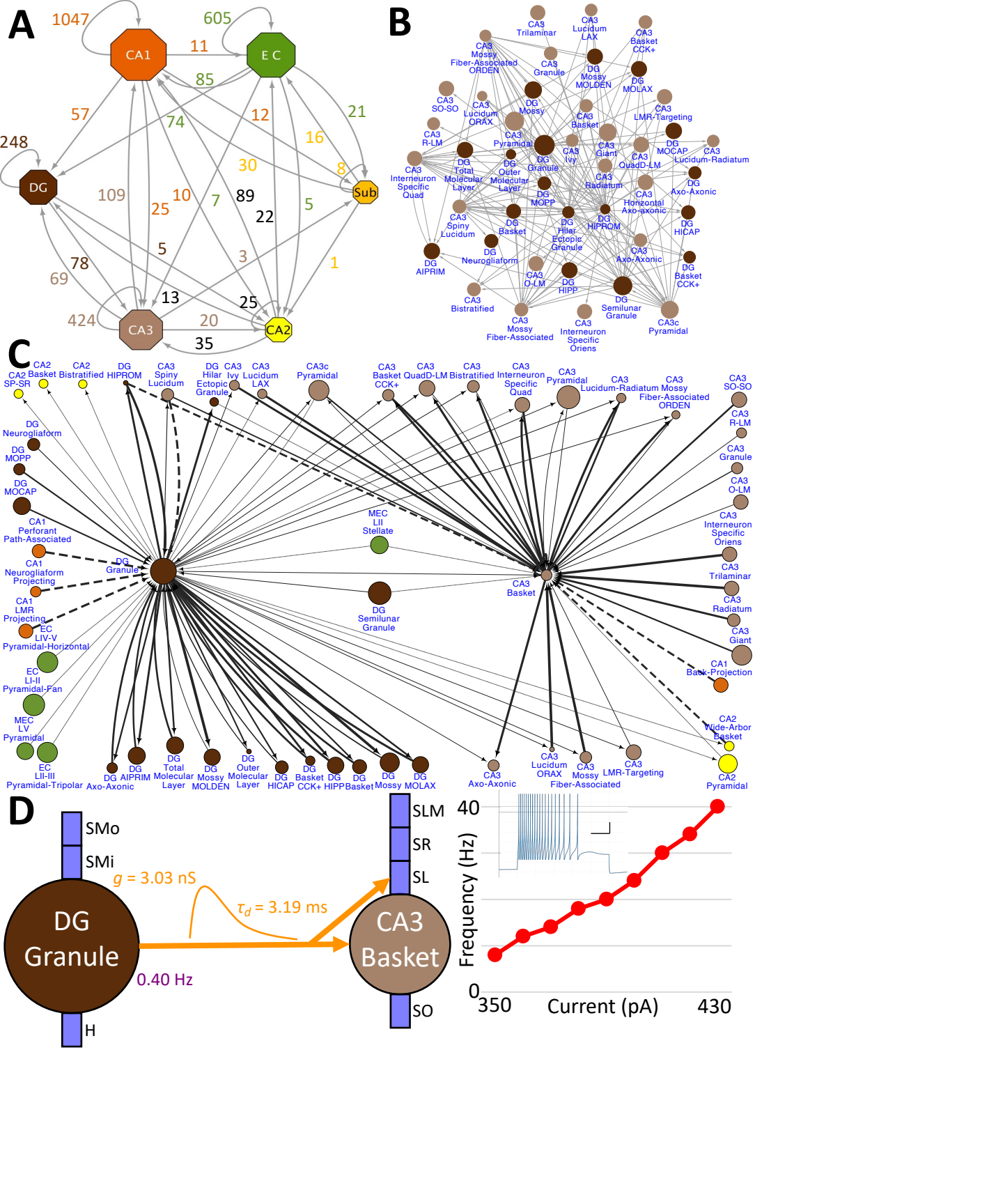
A
CA1
E C
DG
Sub
CA3
CA2
1047
605
11
85
57
74
12
21
248
16
30
8
109
10
7
89
25
22
5
5
3
1
78
69
13
25
424
20
35
B
C
D
SMo
SMi
g = 3.03 nS
τd = 3.19 ms
DG Granule
0.40 Hz
H
SLM
SR
SL
CA3 Basket
SO
40
Frequency (Hz)
0
350
Current (pA)
430

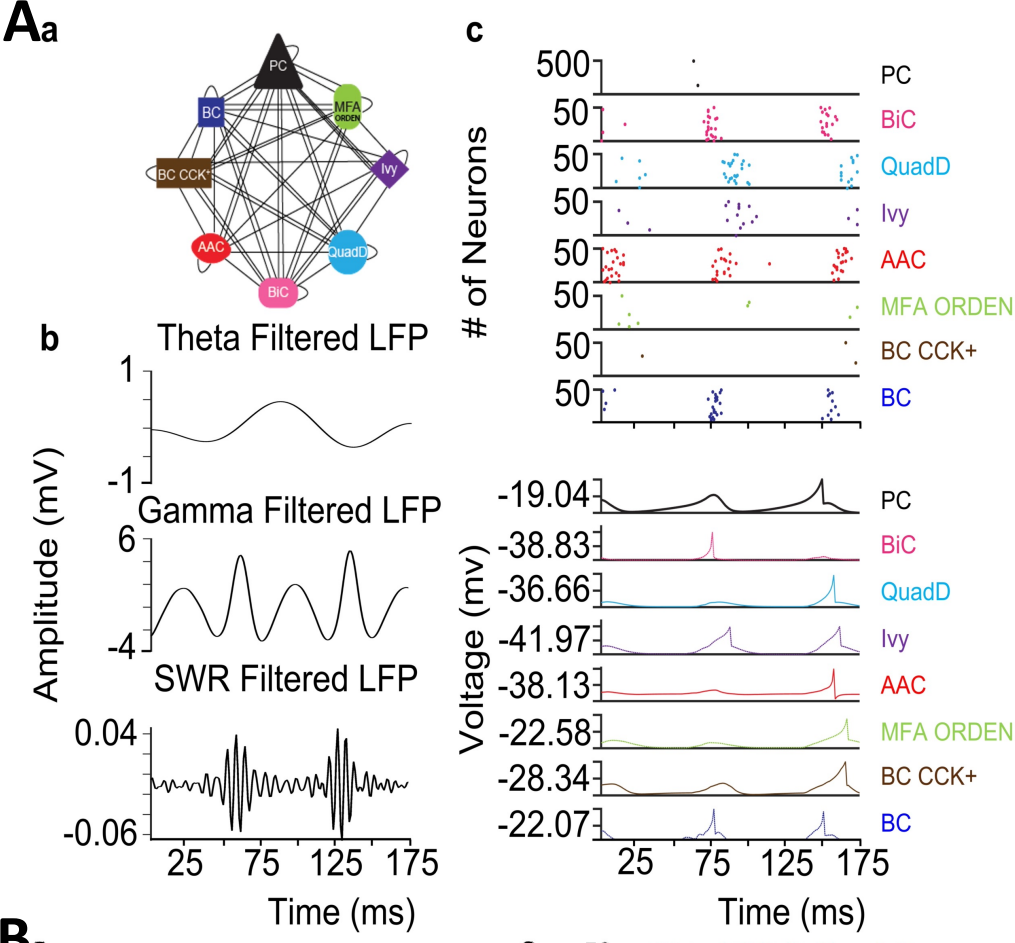
Aa
PC
BC
MFA ORDEN
BC CCK+
Ivy
AAC
QuadD
BiC
b
Theta Filtered LFP
1
-1
Gamma Filtered LFP
6
-4
SWR Filtered LFP
0.04
-0.06
Amplitude (mV)
25
75
125
175
Time (ms)
c
# of Neurons
500
50
PC
BiC
QuadD
Ivy
AAC
MFA ORDEN
BC CCK+
BC
Voltage (mv)
-19.04
-38.83
-36.66
-41.97
-38.13
-22.58
-28.34
-22.07
Time (ms)

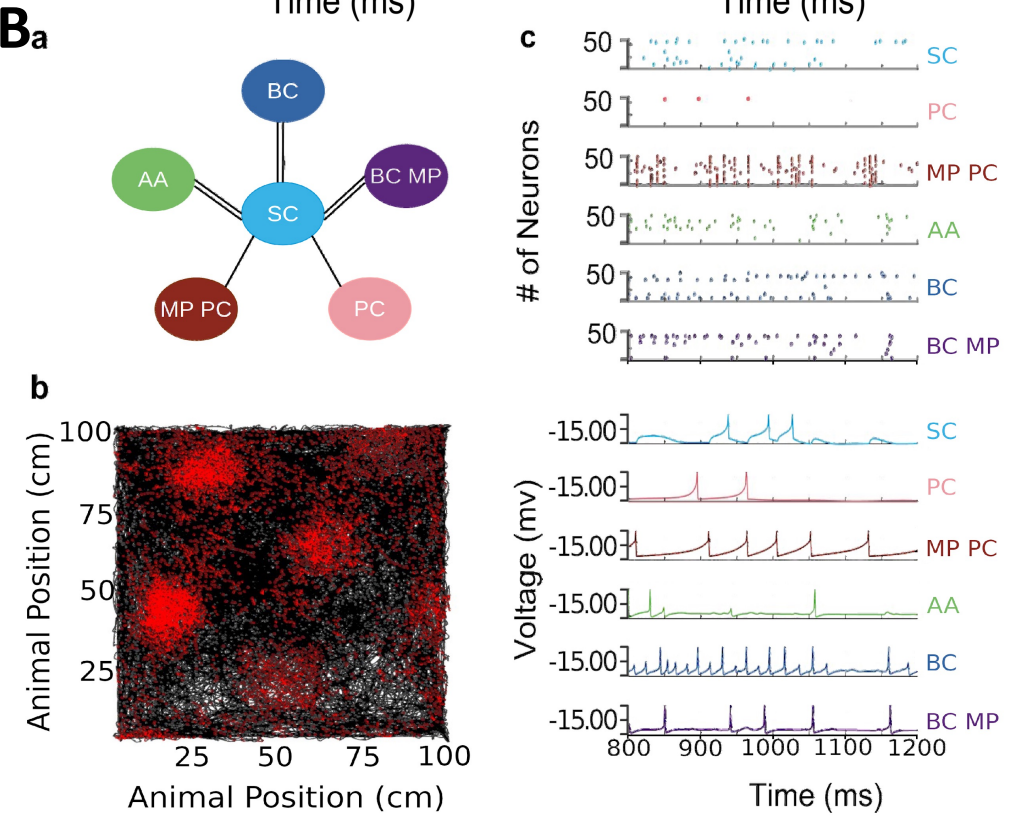
Ba
BC
AA
BC MP
SC
MP PC
PC
b
Animal Position (cm)
100
75
50
25
Animal Position (cm)
c
# of Neurons
50
SC
PC
MP PC
AA
BC
BC MP
Voltage (mv)
-15.00
800
900
1000
1100
1200
Time (ms)